DESIGN AND ANALYSIS OF ALL OPTICAL DIELECTRIC CYLINDRICAL NANOANTENNAS

A Dissertation submitted towards the partial fulfillment of
the requirement for the award of degree of

Master of Technology in
Microwave and Optical Communication Engineering

Submitted by
Inder Devi
2K14/MOC/08

Under the supervision of
Dr. Yogita Kalra
Assistant Professor

Department of Applied Physics and Department of Electronics & Communication Engineering

Delhi Technological University
(Formerly Delhi College of Engineering)

JUNE 2016

DELHI TECHNOLOGICAL UNIVERSITY

Established by Govt. of Delhi vide Act 6 of 2009
(*Formerly Delhi College of Engineering)*
SHAHBAD DAULATPUR, BAWANA ROAD, DELHI-110042

CERTIFICATE

This is to certify that the work which is being presented in the dissertation entitled "**Design and Analysis of All Optical Dielectric Cylindrical Nanoantennas**" is the authentic work of **Inder Devi** under my guidance and supervision in the partial fulfillment of requirement towards the degree of Master of Technology in Microwave and Optical Communication Engineering jointly run by Department of Applied Physics and Department of Electronics and Communication in Delhi Technological University during the 2014-16.

As per the candidate declaration this work has not been submitted elsewhere for the award of any other degree.

Dr. Yogita Kalra (Supervisor)
Assistant Professor
Applied Physics Department
Delhi Technological University (DCE)

Prof. S.C. Sharma
(Head of Department)
Applied Physics Department
Delhi Technological University (DCE)

Prof. Rajesh Rohilla
(Acting Head of Department)
Electronics and Communication Dept.
Delhi Technological University (DCE)

DECLARATION

I hereby declare that all the information in this document has been obtained and presented in accordance with academic rules and ethical conduct. This report is my own, unaided work. I have fully cited and referenced all material and results that are not original to this work. It is being submitted for the degree of Master of Technology in Microwave and Optical Communication Engineering at Delhi Technological University. It has not been submitted for any degree or examination in any other university.

Inder Devi
M. Tech, MOCE
2K14/MOC/08

ABSTRACT

In this thesis, we theoretically demonstrate ultra-directional, azimuthally symmetric forward scattering by dielectric cylindrical nanoantennas for futuristic nanophotonic applications in visible and near-infrared regions. Electric and magnetic dipoles have been optically induced in the nano-cylinders at the resonant wavelengths. It has been demonstrated that the cylindrical dielectric nanoparticles exhibit complete suppression of backward scattering and improved forward scattering at first generalized Kerker's condition. The influence of gap between nano-cylinder elements on the scattering pattern of the homodimers has been demonstrated. Further, for highly directive applications a linear chain of ultra-directional cylindrical nanoantenna array has been proposed.

The effect of the dimensions and material of the dielectric nanocylinder on the scattering properties of the cylindrical nanoantenna has been analyzed using finite element method (FEM). It has been observed that the scattering characteristics of dielectric cylindrical nanoantennas are highly dependent on the dielectric material and aspect ratio of nanocylinder. It has been demonstrated that as dielectric permittivity of the nanocylinder decreases the gap between electric and magnetic resonance decreases hence the directivity increases. We have analyzed that the variation in diameter of nanocylinder has great influence on the strength of interference of electric and magnetic dipolar resonances. As the radius of the nanocylinder is increased, the electric and magnetic dipolar resonances shift towards the higher wavelengths, however no significant change has been observed with the increase in height. Thus, the cylindrical nanoparticles can be used for the design and development of tunable unidirectional nanoantenna applications in visible to near infra-red range

Keywords: tunable, electric resonance, magnetic resonance, dielectric nanoantenna, kerker's condition, directional scattering.

LIST OF RESEARCH PRESENTATION AND PUBLICATIONS

JOURNAL PUBLICATION

- Inder Devi, Reena, Yogita Kalra and R.K. Sinha, "Design and Modeling of All Dielectric Cylindrical Nanoantennas, *Journal of Nanophotonics*, 2016 (Under Review).

CONFERENCE PUBLICATIONS

- Inder Devi, Reena, Yogita Kalra and R.K. Sinha, "Design of tunable cylindrical dielectric nanoantenna", paper accepted for SPIE Conference, 9919-1 (San Diego, September 2016)
- Co-author in paper , "Multipolar optically induced electric and magnetic resonances in the ellipsoidal nanoparticles", with authors Reena, Yogita Kalra and R.K. Sinha accepted for SPIE Conference, 9919-26 (San Diego, September 2016)

ACKNOWLEDGEMENT

The thesis work is a result of hard work and contribution of many well wishers, whose support and guidance has resulted in timely completion of project.

I would like to express my deepest gratitude to my supervisor **Dr. Yogita Kalra**, Asst. Professor, Department of Applied Physics who accepted request of being my guide and for her invaluable support, quality guidance, priceless knowledge and constant motivation throughout the period of the project that has helped in timely completion and submission of this thesis. I am especially grateful to **Dr. R.K. Sinha** not only for giving me interesting ideas and sharing his knowledge, but also for his advice, supervision and patience during the course of this project.

I would like to thank Reena Dalal, research scholar for her valuable time and interest in the project. Her knowledge, advice and time bound solutions for the queries raised during the course of the project have helped me in timely completion of the project work

I am deeply grateful to **Prof. S.C. Sharma**, H.O.D (Dept of A.P.), **Prof. Prem R. Chadha**, H.O.D (Dept. of ECE), **Prof. Rajiv Kapoor**, **Dr. Ajeet Kumar** for their support for providing us with all the facilities to carry out quality project work.

I also would like to thank all the members from the SPIE DTU Student Chapter group, at the Applied Physics department, for their help and advice. In particular, I thank Nishant Shankhwar, Preeti Rani, Kamal Kishor, Than Singh Saini and Neeraj Sharma for being always willing to answer and discuss any question. Without them, my job would have undoubtedly been more difficult.

I also wish to express my heart full thanks to the classmates as well as staff at Department of Applied Physics and Department of Electronics and Communication of Delhi Technological University for their goodwill and support that helped me a lot, in successful completion of this project.

Finally, I want to thank my parents, for inculcating good ethos, as a result of which I am able to do my post-graduation from such an esteemed institution. I would thank my friends for believing in my abilities and for always showering their invaluable support and constant encouragement.

Inder Devi
M.Tech. MOCE
2K14/MOCE/08

LIST OF CONTENTS

LIST OF FIGURES

CHAPTER 1

INTRODUCTION

1.1 Thesis Motivation and Approach

Optical nanoantennas refer to the objects or elements used for reception and transmission of optical signal. The optical nanoantennas are basically of two types-plasmonic and dielectric nanoantennas. The dielectric nanoantennas present sharp resonances and have low dissipative losses in visible and near-infrared regions as compared to its plasmonic nanoantennas. These interesting advantages over metallic counterparts make dielectric nanoantennas as popular choices for directional scattering in visible and near-infrared regions. This dissertation consists of a design of ultra-directional, all-dielectric cylindrical optical nanoantenna. The cylindrical dielectric nanoantennas support azimuthally symmetric forward scattering for futuristic nanophotonic applications in visible and near-infrared regions. A dielectric nanoparticle supports both electric and magnetic resonances. The forward scattering by dielectric nanoparticle is observed at first generalized Kerker's condition. The scattering properties of the dielectric nanoantennas are analyzed using Finite Element Method in COMSOL MULTIPHYSICS software. The influence of gap between nanoantenna homodimers has been also studied. Further, the effects of nanoparticle parameters on scattering properties of dielectric nanoantennas are also investigated.

1.2 Thesis Objective

The main objectives of the thesis are as follows:

- To study the basic concepts of optical nanoantennas, its characteristics, types and nanoantenna applications. Further, to study the recent advancements in the field of dielectric optical nanoantennas.
- To learn the numerical techniques to model nanoantennas i.e. Finite Element Method.
- To design and modeling of a new dielectric nanoantenna structure i.e. cylindrical dielectric nanoantenna for futuristic nanophotonic applications in visible and near-infrared region.

- To study the scattering properties of all-dielectric cylindrical nanoantenna in detail. Further, to study the influence of gap between nanoantenna elements on scattering pattern of the homodimers.
- To study the effect of nanoparticle material and parameters on the scattering properties of the all-dielectric cylindrical nanoantennas.

1.3 Thesis Organization

The rest of the report is organized as follows:

Chapter 2 includes the literature review of the research papers and survey papers that were studied during the course of the project. In this chapter optical nanoantennas have been discussed in detail. Further, two types of optical nanoantennas-plasmonic and dielectric nanoantennas were discussed.

Chapter 3 includes the calculational method and tools used for design and analysis of the cylindrical nanoantenna.

Chapter 4 includes the design, simulations and results of the proposed dielectric structure. This chapter covers the detailed analysis of scattering properties of the proposed design. The influence of gap in nanoantenna array and increase in directivity with number of nanoantenna elements is also discussed in this chapter.

In chapter 5, the effects of dielectric permittivity and design parameters on the scattering properties of the nanoantenna structure are discussed.

Chapter 6 discusses the conclusions withdrawn from the results obtained and the future scope in the direction of the project.

CHAPTER 2

OPTICAL NANOANTENNAS

Optical nanoantennas have been a topic of great interest in many applications from near-field microscopy to molecular and biomedical sensors, optical communication, solar cells and optical tweezers [1-7]. The field of optical nanoantennas is a rapidly developing area of optics. There are many optical nanoantennas designed for nanophotonic applications. Nanoantennas are classified into two types i.e. metallic and dielectric. The history of the development of nanoantennas started with the work of Edward Hutchinson Synge in 1928, who was the first to suggest using metallic nanoparticles for optical confinement. After that in 1985, John Wesssel [8] came up with the concept of metallic nanoparticles as an antenna which support surface plasmon resonances. This study was the major step towards the development of nanoantennas. Soon, many plasmonic nanoantennas were designed which can radiate in the desired direction according to the requirements. The main types of plasmonic nanoantennas are monopole, dimer, yagi-uda and rhombic [9]. Dipole nanoantennas demonstrate high coefficient of electric field localization [10], while bowtie nanoantennas are broadband. Plasmonic nanoantennas continue to improve and new designs are proposed from time to time. However, the biggest drawback of these nanoantennas, including high energy dissipation, motivated towards the search for new solutions. To overcome such limitations the high dielectric antenna structures were designed. In [11] for the first time authors, experimentally demonstrated directional light scattering by spherical silicon nano particle in the visible range. The phenomenon was similar to Kreker-type scattering predicted in [12] for hypothetical magneto-dielectric nanoparticles. In [13], the authors introduced the concept of all dielectric nanoantennas employed in Yagi-Uda geometry using dielectric nanospheres, which exhibits both electric and magnetic resonances resulting in narrow radiation pattern and high directivity. These unique properties of high refractive index dielectric nanostructures constitute the background for all the advances in dielectric nanoantennas.

2.1 Introduction

Antennas are the most important elements of modern radio and microwave frequency communication technologies. Antennas refer to the devices converting electric current into the propagating radio waves and, vice versa [14]. Recently, due to the development in the field of nano-optics, a new branch of physics, the concept of the antennas has been extended to optical range. The nano-optics deals with the transmission and reception of optical signals by small objects of submicron and even nanometer size. The major problem in nano-optics is the directivity and efficiency of the transmission of optical signals between the nano-objects. These nano-objects used for transmission and reception of optical information are known as optical nanoantennas.

The physics of optical nanoantenna and radio frequency antennas are different in two important aspects that are, first, due to very high losses at optical frequencies, the assumption of perfect electrical conductor is no longer valid; and second, due to unique phenomena at nanoscale level, e.g., surface plasmon polaritons (SPP), the response of these structures can be quite different from the radio frequency structures.

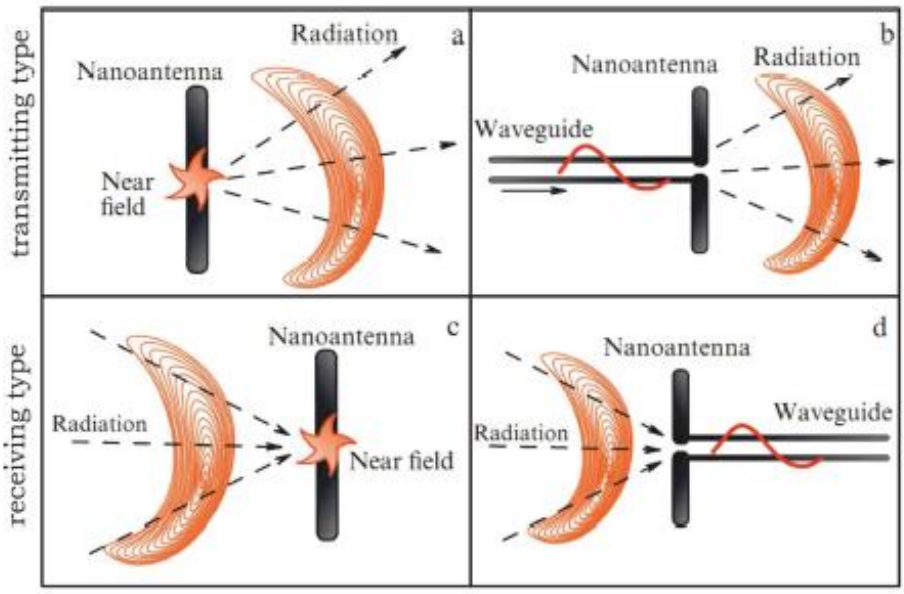

Fig. 2.1 The basic principles of nanoantenna operation. (a, b) Transmitting nanoantenna- the waveguide mode and transformation into freely propagating optical radiation; (c, d) explains a reception process [15].

The term optical nanoantennas refer to the devices effectively converting optical frequency radiation into strongly confined field and, vice versa. Nanoantenna elements must exhibit high directivity and radiation efficiency. The basic principle of nanoantenna operation is as shown in figure 2.1. The optical nanoantennas are divided into two types that is transmitting and receiving antennas. The property of transmitting antenna is to convert the strongly confined field in the optical frequency radiation. Figures 2.1(a,b) show how transmitting nanoantenna interacts with the emitter and converts near field into optical radiation. Figures 2.1(c,d) show the receiving nanoantenna operation, for reception nanoantenna converts incident radiation into a strongly confined near field. The energy received by nanoantenna is delivered to microwave antenna through waveguide. The waveguides used in optical communication are known as plasmonic waveguides. The optical nanoantennas are basically of two types, plasmonic and dielectric nanoantenna. The construction of optical nanoantennas started with metallic materials which support the plasmonic resonances.

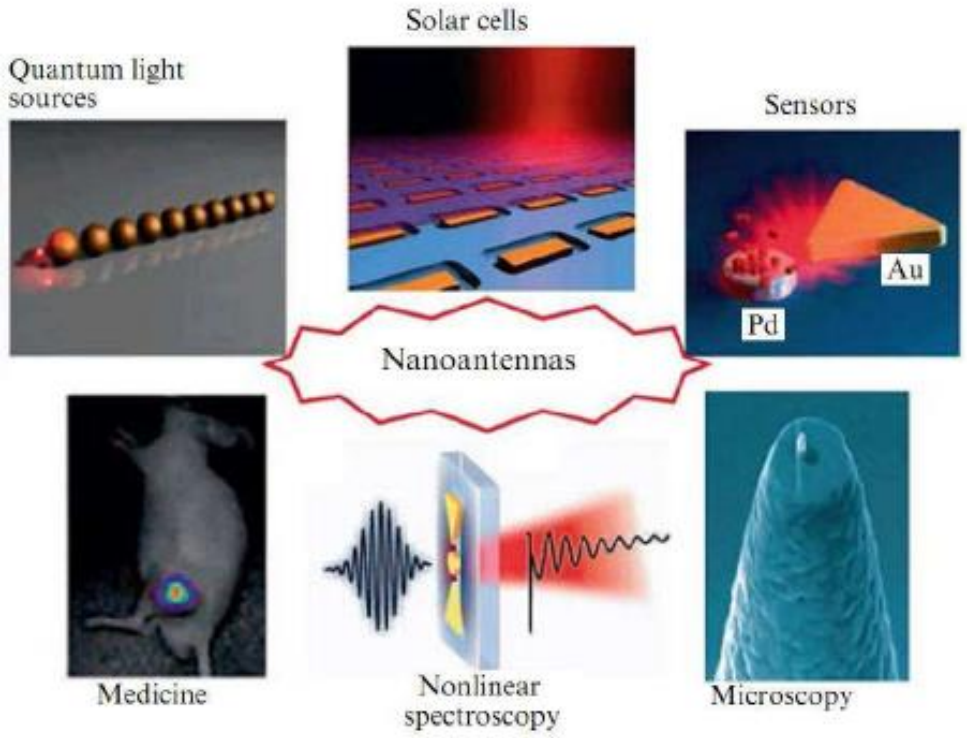

Fig. 2.2 Nanoantennas application in modern science [15].

2.1.1 Applications of optical nanoantennas in modern science

Optical nanoantennas are most promising area of research in the nano-optics. Nanoantennas bridge the size mismatch and impedance mismatch between nano-emitters and free space radiation. Nanoantennas have many promising applications in near-field spectroscopy, high-resolution molecular and biomedical sensors, solar cells, optical communication and optical tweezers as shown in figure 2.2.

Research in the field of optical antennas has variety of possible applications that have great advantages to enhanced light-matter interaction. Till now most of the applications have been discussed in reviews of plasmonics and optical antennas [16-20]. Optical nanoantennas have a vast number of nanophotonic applications. In this section we will highlight the some important nanoantenna applications.

i. Scanning near-field optical microscopy:

Near field optical microscopy provides simultaneous measurements of the topography and optical properties (fluorescence). Nanoantennas have been proposed as imaging and spectroscopic probes which help in light passage through the probe aperture and to enhance the effect of electromagnetic field near the tip of a aperture less probe. Nanoantennas need to be fabricated at the tip of a scanning probe. An interesting example of near field spectroscopy is a single-molecule imaging which has been achieved with bow-tie [21] and $\lambda/4$ antennas [22], and resolution down to 25 nm can be obtained in the latter case. The optical antennas help us to dramatically increase the efficiency of light passing through aperture probes. It is very difficult to design the probes based on optical nanoantennas because sometimes it is almost impossible to differentiate them on based on presence or absence of the aperture.

The work on probe antennas is mainly focused to enhance the scattering of molecules or quantum emitters. The optical probe nanoantennas are also used in tip-enhanced Raman Spectroscopy which have complicated structures for example, a combination of plasmonic waveguide and a photonic crystal, coaxial structures and carbon nano-tube based structures [23-25].

ii. Spectroscopy:

SERS (Surface enhanced Raman spectroscopy) is the phenomenon in which consist of enlargement of the scattering cross section of the molecule placed near a rough metal surface [26-29].

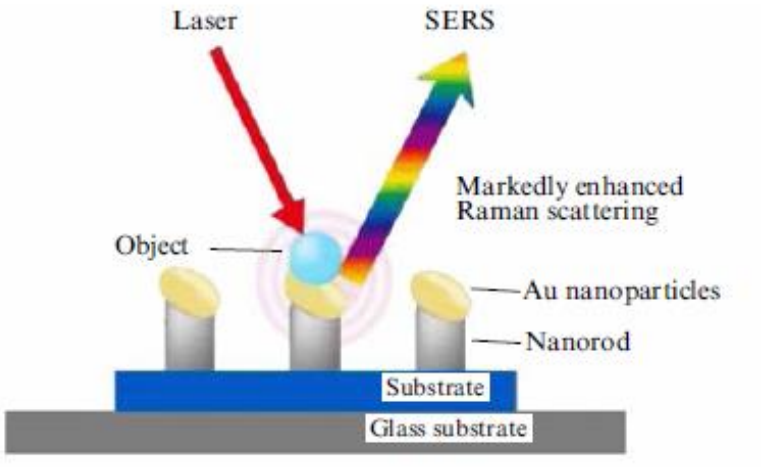

Fig. 2.3 Surface Enhanced Raman Spectroscopy (SERS). (Source: http://www.nidek-intl.com)

The history of spectroscopy started in an experiment in 1970s. The application of this effect was to creation of substrates to study the biological samples. The signals can be largely enhanced following the surface-enhanced and tip-enhanced Raman scattering as shown in figure 2.3 [30, 31]. The Raman scattering involves the absorption and emission of photons which are nearly identical in energy. The total scattering enhancement is usually proportional to the fourth power of the field enhancement. Hence, typical enhancement factors obtained are $\approx 10^6$, and it is possible to obtain factors as large as $\approx 10^{10}-10^{12}$. Such enhancement enables the detection of single molecules [32].

iii. Optical lithography

The highly localized near field of a nanoantenna also finds a natural application in optical lithography. Lithography is a process to create a resist image on a given wafer. It is the important part of semiconductor manufacturing technology.

Optical lithography consists of an optical system which transfers the image from the mask to the resist layer. The plasmonic dimers for example bow-tie antenna confined the field to a limit where it is equivalent to a strong light spot which will improve the resolution of optical lithography [33]. The process of optical lithography is shown in figure 2.4 and the effective source used is optical nanoantenna.

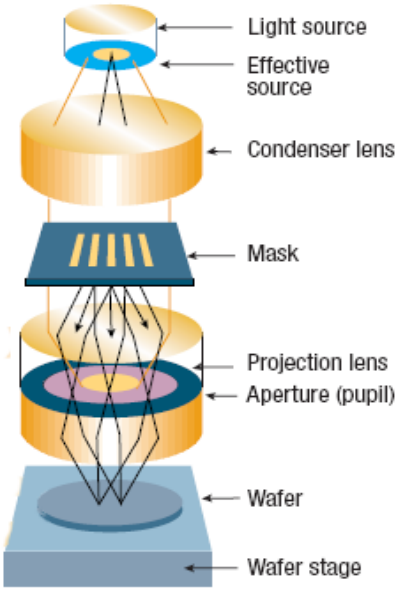

Fig. 2.4 The process of optical lithography [34].

iv. Optical tweezing with nanoantennas

Optical tweezers are the instruments that use light to manipulate microscopic objects as small as a single atom [35]. More recently, it has been demonstrated experimentally that the optical trapping in well-controlled hot spots in the gap of nanoantennas. The large antenna field enhancement allows trapping with lower excitation power and higher efficiency and stability [36,37].

v. Antenna-based photovoltaics:

The problem with modern solar power engineering is the development of thin film solar cells which can efficiently convert solar radiation into electric current. The use of thin photosensitive films in solar cells may reduce the cost of electric power with a significant magnitude. Plasmonic photovoltaics is one of the most recent fields in nanophotonics which can confined incident radiation in subwavelength range [38]. Standard solar cells are combined with metallic nanostructures, which concentrate and guide light at the nanoscale, leading to a reduction of the semiconductor thickness required, as well as enhancing the broadband absorption of the incident light, which is one of the crucial challenges to modern solar cell technologies [39].

vi. Optical antenna sensors

Plasmonic nanoantennas exhibits localized resonances that are strongly depend on dielectric properties of the environment. These type of nanoantennas are very promising candidates to

sensing application. The basic principle behind plasmonic sensing is that the refractive index change in the surrounding medium of the nanoantenna translates into a shift of particles resonance frequency. Many plasmonic sensors were demonstrated in past for example, sensing based on particle arrays on a fiber facet [40] or on a substrate [41] with sensitivities down to the single-particle level [42, 43].

vii. Lasing in nanoantennas

Surface plasmon amplification by stimulated emission of Radiation (SPASER), has been originally proposed by Bergman and Stockmann [44]. In this context, metal nanoparticles acting as optical antennas can play a role because of their large local field enhancement and extremely reduced interaction volume. Very recently, subwavelength plasmon lasers based on the original SPASER proposal have been demonstrated [45, 46]. Larger enhancement and confinement, compared to single particles, can especially be encountered in the gap of two-wire or bow-tie nanoantennas. Along this line, laser operation for bow-tie antennas coupled to semiconducting quantum dots or multiple quantum wells has been theoretically addressed [47].

viii. Nanomedicine

The use of metal nanoparticles for biomedical applications has resolved many challenges in modern medicine [48, 49]. Nanoparticles can be used in therapy for malignant neoplasms. Metallic nanoparticle placed at the affected site is irradiated with the near field light, the heating of nanoparticle causes by radiation is transferred to cancel cells and thereby kill them. The imaging of biological samples and the detection of diseases such as cancer require biomarkers and contrast agents. There is an interest in exploiting the large scattering cross sections associated with LSPRs for bio-imaging and drug and gene delivery [50]; application which rely on both their biostability and optical properties. Gold particles have also been proposed as contrast agents for magnetic resonance imaging [51]. The absorptive properties of metal NPs are also promising for medical imaging [52].

2.1.2 Types of Optical nanoantennas

Optical nanoantennas are primarily constructed of metallic materials, known as metallic nanoantennas or plasmonic nanoantennas. In metallic nanoantennas, a metallic nanoparticle behaves as an antenna. The antenna behavior of metallic nanoparticle is due to the ability to support surface plasmonics. Plasmonics is the branch of nanophotonics which studies how the electromagnetic field can be confined over a dimension of order smaller than the wavelength.

The quantization of collective longitudinal excitation of a conductive electron gas in a metal is known as plasmon. In simple words a plasmon is the quantum of plasma oscillation. The interaction of an electron passing through a thin metal surface is required to excite the plasmon. An enhanced optical near field is achieved when the electromagnetic field interacts with the conductive electrons at the metal interface. The metallic nanoparticle has ability to enhance the electromagnetic field strength upon excitation of plasmon resonances that is why it is also known as plasmonic nanoantenna.

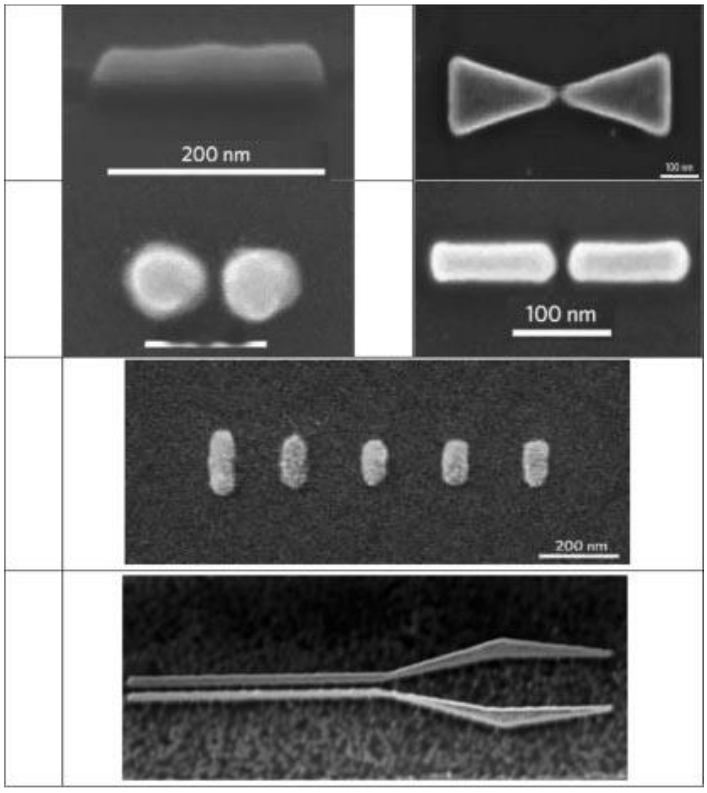

Fig.2.5 Main types of plasmonic nanoantennas [15]

There are many plasmonic nanoantennas structures constructed for different applications as shown in figure. 2.5. For example dipole nanoantenna structures demonstrate high coefficient of electric field localization, while bowtie nanoantennas are broadband; Yagi-Uda type nanoantennas exhibit high directivity which is very useful for optical wireless communications. However, despite of a number of advantages of plasmonic nanoantennas such as their small size and strong localization of the electric field, such nanoantennas have large dissipative losses resulting in low radiation efficiency.

A new type of nanoantennas were proposed, to overcome the limitations of plasmonic nanoantennas, based on the principle of dielectric nanoparticles with a high index dielectric constant such as Huygens optical elements and Yagi-Uda nanoantennas. All-dielectric optical nanoantennas have low dissipative losses and enhanced magnetic response in the visible region. The key for such novel functionalities of high index dielectric nanophotonic elements is the ability of dielectric nanoparticles to support both electric and magnetic resonances simultaneously, which also can be controlled independently. This type of nanoantennas has several unique features such as low optical losses at the nanoscale and super directivity.

2.1.3 Basic characteristics of optical nanoantennas

The optical nanoantennas are characterized on the basis of different antenna parameters. The main parameters of nanoantennas are explained below.

i. Directivity:- A primary characteristic of any antenna (or nanoantenna) is its directivity. Directivity of an antenna defined as "the ratio of the radiation intensity in a given direction from the antenna to the radiation intensity averaged over all directions. The average radiation intensity is equal to the total power radiated by the antenna divided by 4π. If the direction is not specified, the direction of maximum radiation intensity is implied." The directivity diagram is a real positive function coinciding in the spherical coordinate system with the Poynting vector distribution in the far radiation zone. For an antenna, the concentration of radiation in a particular direction is given by the directivity. The standard definition of directivity is given by the expression [53]

$$\boldsymbol{D(\theta,\varphi) = \frac{4\pi p(\theta,\varphi)}{P_{rad}}} \qquad (2.1)$$

Where P_{rad} is the total power radiated by the system, $\int p(\theta,\varphi)d\Omega$, is the integral of the angular distribution of the radiated power $p(\theta,\varphi)$ over the spherical surface, where (θ,φ) are the angular coordinates of the spherical coordinate system, and $d\Omega$ is the element of the solid angle. The directivity of an antenna tell us how many times the radiated power should be increased when a directional antenna is replaced by an absolutely non-directional one. The maximum value of directivity is given by

$$\boldsymbol{D_{max} = \frac{4\pi Max[p(\theta,\varphi)]}{P_{rad}}} \qquad (2.2)$$

Where, Max p(θ,φ) is the power transmitted in the direction of the main lobe.

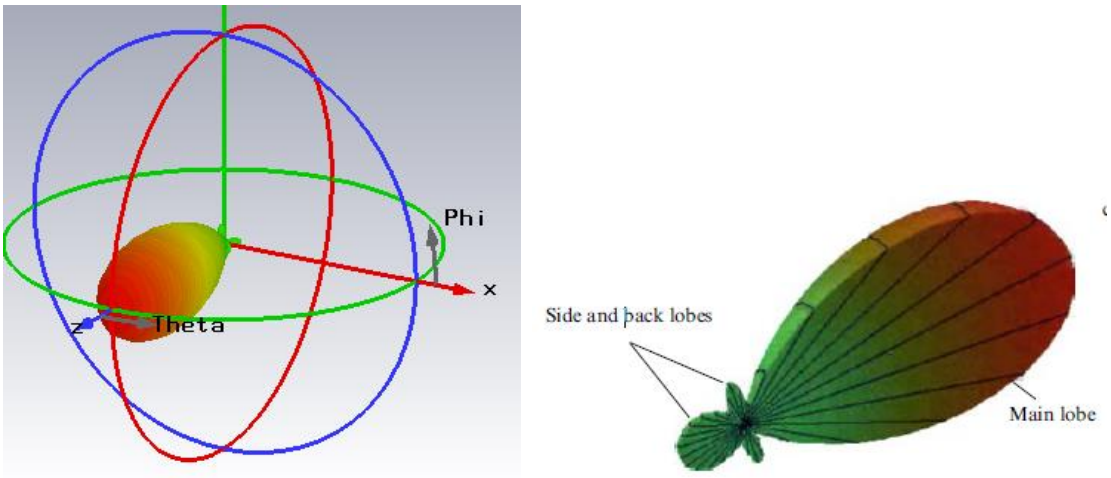

Fig. 2.6 Directivity diagrams for a yagi-uda nanoantenna.

ii. Efficiency:- The antenna efficiency that takes into account all the reflection, conduction, and dielectric losses. The conduction and dielectric losses of an antenna are very difficult to compute and in most cases they are measured. Even with the help of measurements, they are very difficult to separate. Hence, they are generally lumped together to form the radiation efficiency of an antenna.

$$\boldsymbol{\varepsilon_{rad}} = \frac{\boldsymbol{P_{rad}}}{\boldsymbol{P_{rad}+P_{loss}}} \qquad (2.3)$$

where P_{loss} is the total power loss in the material of the nanoantenna. For a lossless antenna, one has radiation efficiency, $\varepsilon_{rad} = 1$.

The maximum value of the gain is related to the maximum directivity of by

$$G = \boldsymbol{\varepsilon_{rad}} \boldsymbol{D} \qquad (2.4)$$

This quantity defines directivity, taking account of losses in the antennas.

iii. Absorption cross section of a quantum detector (Field factors):- Quantum detectors used in the optical frequency region have subwavelength spatial dimensions. The quantum detectors are characterized by a small absorption cross section σ equal to the ratio of the absorbed power P_{exc} to incident radiation intensity :

$$\boldsymbol{\sigma(\theta, \varphi. n_{pol}) = \frac{P_{exc}}{I}} \quad (2.5)$$

Where, n_{pol} is the direction of polarization of the incident field E.

For a detector which is described using dipole approximation, the absorption cross section can be written as [15]

$$\boldsymbol{\sigma = \sigma_0 \frac{(n_p E)^2}{(n_p E_0)^2}} \quad (2.6)$$

Where, σ_0 is the absorption cross section in the absence of a nanoantenna, n_p is the orientation of the absorbing dipole, and E and E_0 are the electric field strengths in the presence and absence of the nanoantenna, respectively. Nanoantennas has ability to enhance the near field in a certain space region, hence the absorption cross section of a detector placed in this region is also gets enlarged.

iv. Confined electric and magnetic field enhancement factors:- The absorption cross section of a detector also depends on the enhancement factor of the confined electric field, which is given by

$$\boldsymbol{\delta^e = \frac{|E|}{|E_0|}} \quad (2.7)$$

Where, |E| is the absolute strength of the electric field at a given point in the presence of a nanoantenna and $|E_0|$ is the absolute strength of electric field in the absence of a nanoantenna. The enhancement factor coefficient may be either greater or less than unity. For practical applications, it must be greater than unity because only in such case the detector efficiency increases in the presence of the nanoantenna.

v. Purcell effect:- Before EM Purcells [54] work, it was assumed that the spontaneous radiation is an intrinsic property of molecules or atoms. Hence, the spontaneous radiation of the molecule or atoms cannot be modified. Purcell showed in his work that the spontaneous relaxation rate depends partly on the environment of a light source, thus suggesting that by placing light source in a special environment the emission properties of the an atom and emitter can be modified.

An emitter has its own spectrum of energy states. All these energy states are stationary, and when an emitter is excited into one of these states it must remain in that state for

infinitely long. However, an emitter in the excited state is characterized by a finite or short lifetime due to its interaction with the environment. For example, in the simple scenario of a single emitter, the surrounding medium is the free space. The rate of spontaneous emission depends partly on the environment of a light source. This means that by placing the light source in a special environment, the rate of spontaneous emission can be modified. This effect was called the Purcell effect.

The Purcell factor F_P is given by the spontaneous emission rate of the emitter placed in a certain heterogeneous system, γ, compared with the spontaneous emission rate in the free space, γ_0.

$$\boldsymbol{F_P = \frac{\gamma}{\gamma_0} = \frac{P_{tot}}{P^0}} \qquad (2.8)$$

The Purcell factor is also related to the variation of the total power P_{tot} radiated by the emitter compared to the power P^0 that the emitter radiated in the free space. The process of enhancement of spontaneous emission depends on the variation of the number of excitation acts and spontaneous emissions of the emitter per unit time. The total power P_{tot} is define as the sum of two powers, one radiated by the system, and absorbed in the material of the nanoantenna and its external environment.

2.2 Dielectric nanoantennas

Dielectric nanoantennas are the optical nanoantennas design using the dielectric nanoparticles which support both the electric and magnetic resonances. Such dielectric nanoantennas have low dissipative losses. In last few years, the dielectric nanoantennas designs are exhibiting advantages over metallic nanoantennas. Dielectric nanoantennas are fabricated using optically transparent materials such as semiconductor and dielectric materials. All–dielectric nanoantennas are of great interest to researchers due to their unique properties. Dielectric materials exhibit electric and magnetic resonant responses simultaneously. This property of dielectric materials makes possible the creation of Huygens element using a single dielectric particle. Huygens particles have the directional properties and low losses. Many nanoantenna structures can be constructed using Huygens elements, for example, yagi-uda nanoantennas.

2.2.1 Huygens element

The concept of Huygens element is based on the Huygens principle. According to Huygens principle, "all points of a wave front of light in a vacuum or transparent medium may be regarded as new sources of wavelets that expand in every direction at a rate depending on their velocities**".** Proposed by the Dutch mathematician, physicist, and astronomer,Christiaan Huygens, in 1690, it has become a powerful method for studying various optical phenomena. Huygens principle of wave analysis helps understand the movements of waves around objects [55].

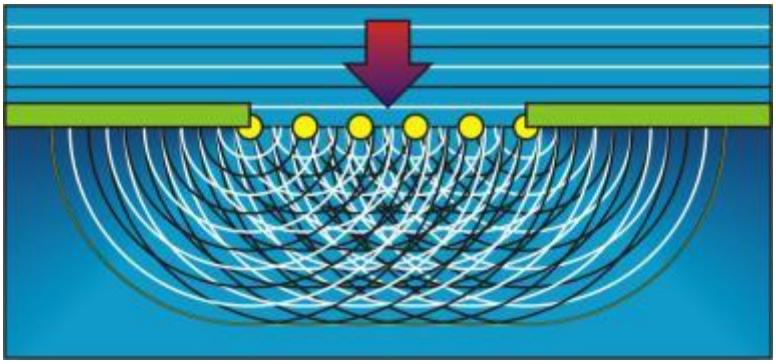

Fig 2.7 Illustration of Huygens principle. (source: http://www.britannica.com/science/Huygens-principle)

As shown in the figure 2.7 to the right, when light goes through an aperture (an opening within a barrier) every point of the light wave within the aperture can be viewed as creating a circular wave which propagates outward from the aperture.

The aperture, therefore, is treated as creating a new wave source, which propagates in the form of a circular wave front. A surface tangent to the wavelets constitutes the new wave front and is called the envelope of the wavelets. If a medium is homogeneous and has the same properties throughout (*i.e.,* is isotropic), permitting light to travel with the same speed regardless of its direction of propagation, the three-dimensional envelope of a point source will be spherical.

Huygens element is a dielectric particle of high permittivity material i.e. in order of 10-20. Due to high permittivity of dielectric material first two Mie resonances, electric and magnetic, are observed in visible frequency range [56]. The electric and magnetic moments are induced when excited by an emitter. Huygens particles can be used to design dielectric nanoantennas with high directivity. A Huygens element (of silicon material) is shown in figure 2.8(a). A spherical

dielectric silicon nanoparticle is placed in the near field of an elementary dipole. Figure 2.8(b) depicts the wavelength dependence of the directivity factor for Huygens element.

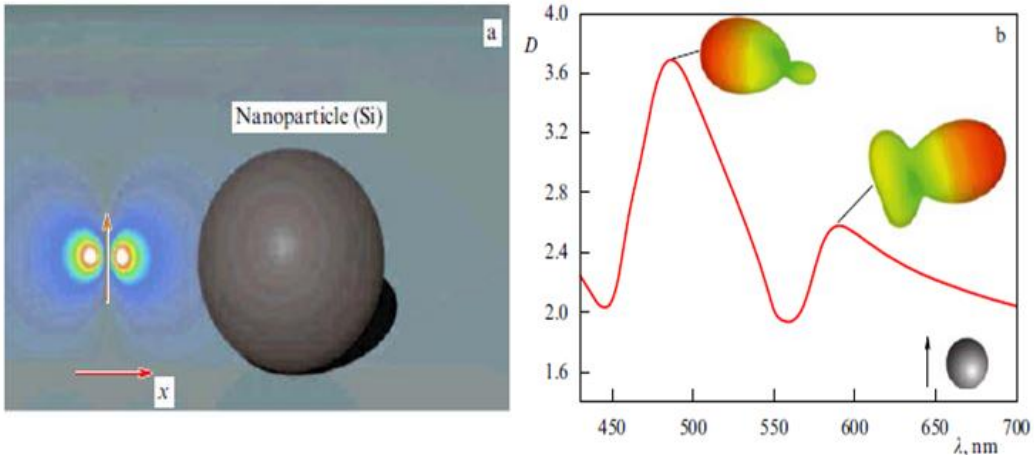

Fig. 2.8 (a) An example of Huygens element. (b) Wavelength dependence of directivity factors [9].

2.2.2 Optical magnetism in Dielectric nanoantennas

An oscillating dipole is referred as a pair of oscillating electric charges of opposite signs. The oscillating dipole produces electromagnetic (EM) radiation at the frequency of oscillations. Single "magnetic charges" or monopoles are not found in nature. The common sources of magnetic field in nature are magnetic dipoles. Magnetic dipole field can be calculated as the limit of a current loop that is shrinking to a point. The common example of a magnetic dipole radiation is an EM wave produced by a split ring resonator as shown in figure 2.9.

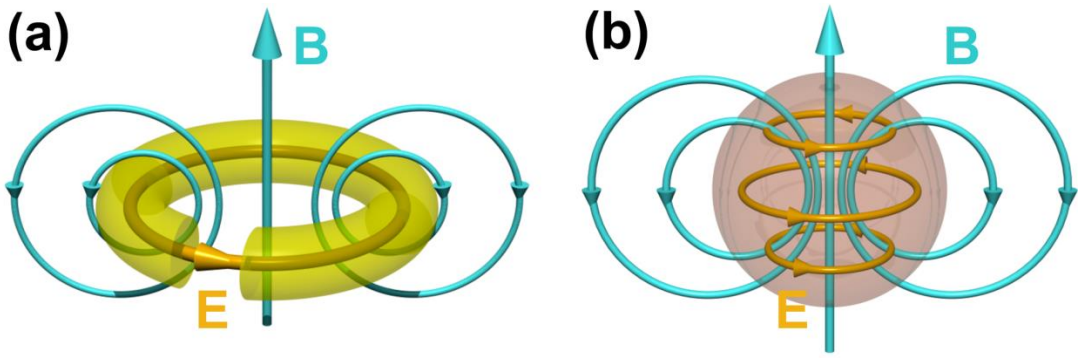

Fig. 2.9 (a) The schematic representation of EM field distribution inside a SRR and high refractive index dielectric nanoparticle. (b) EM distribution at magnetic resonance [57].

The current inside the split ring resonator which is excited by an external EM radiation produces a transverse oscillating up and down magnetic field at the center of the resonator ring, which forms an oscillating dipole. The split ring resonator is the basic element for metamaterials.

The reasons for interest in such artificial systems are as follows:

- They have ability to response to a magnetic component of incoming EM radiation.
- They have magnetic permeability which is either non unity or negative at optical frequencies.
- These types of systems with above properties are not found in nature.

The artificial system have many applications in design of material properties such as clocking [58, 59], superlensing [60], negative refraction [61] etc. However, the biggest disadvantages of metal artificial system are intrinsic losses at visible frequencies. So an alternative to avoid such losses and achieve magnetic response is to use high-refractive index dielectric nanoparticles [62]. The strong magnetic response by high-index dielectric particles is explained using a spherical dielectric nanoparticle. The scattering by a spherical dielectric nanoparticle follows Mie solution of light scattering. For this particle a strong magnetic dipole resonance can be achieved in a particular parameter range. The first resonance of this particle is a magnetic dipole resonance and it take place at wavelength of the light $\lambda/n_s \approx 2R_s$, where λ is wavelength in free space, R_s and n_s are the radius and refractive index of the particle. Magnetic field oscillations in the centre under this condition are as shown in figure 2.9(b).

CHAPTER 3

CALCULATIONAL METHOD AND SOFTWARE TOOLS

3.1 Finite Element Method

3.1.1 Introduction

Partial difference equations (PDEs) are usually arises in science and engineering applications which are used to describe the system problems. For the vast majority of geometries and problems, these PDEs cannot be solved with analytical methods. Instead of that, an approximation of the equations can be constructed, typically based upon different types of discretizations. These discretization methods approximate the PDEs with numerical model equations, which can be solved using numerical methods. The solution to the numerical model equations are, an approximation of the real solution to the PDEs. The finite element method (FEM) is a numerical method used to solve those problems. In this method the domain of interest is represented as an assembly of finite element. A continuous physical problem is transformed into a discrete finite element problem [63].

There are two important features of the FEM which are mention below:

- Piece-wise approximation of physical fields on finite elements which provides good precision even with simple approximating functions. We can achieve any precision increasing the number of elements.
- Locality of approximation leads to sparse equation systems for a discretized problem. This helps to solve problems with very large number of nodal unknowns.

3.1.2 The FEM procedure

The finite element method is a step by step process (as shown in figure 3.1), which are explained below:

1. Discretize the continuum

   The first and foremost step is to divide a solution region into finite elements. The finite element mesh of the solution region is generated by a preprocessor program. Mesh is

generally consists of several arrays which further consist of element connectivities and nodal co-ordinates.

2. Selection of interpolation functions

The Interpolation functions are used to interpose the field variables over the element. The polynomials which are derived equations to satisfy the nodal conditions are selected as interpolation functions. The degree of the polynomial required for interpolation functions depends on the number of nodes assigned to the element.

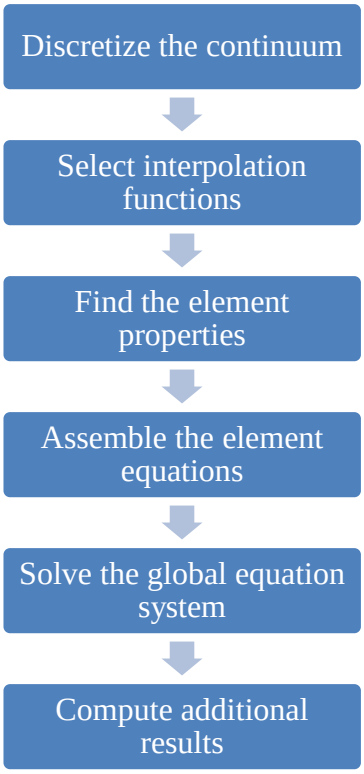

Fig. 3.1 Flow diagram showing step by step procedure of FEM.

3. Find the element properties

The next step is to find the element properties. Here we have to establish the matrix equations for the finite element which will relate the nodal values of the unknown function to other parameters. For this task any convenient approaches can be used; the most convenient approaches used in finite element method are: the variational approach and the Galerkin method.

4. To assemble the element equations

   After establishing matrix equation for finite element, next step is to find the global equation for the whole system. Hence, we must assemble all the element equations to form a global equation system. In other words, we must combine the local element equations for all elements that are used for discretization. For the assembly of the equations the Element connectivities are used. The boundary conditions should be imposed before the solution is obtained because in element equations they are not accounted.

5. Solve the global equation system

   The global equation system formed in previous step is solved using different methods. The finite element global equation system is generally sparse, symmetric and positive definite. To solve the global equation system direct and iterative methods can be used. The nodal values of the required function are produced as a result of the solution of global equation.

6. Compute additional results

   This step is the final step for the finite element method process. In many cases we need to calculate additional parameters as depending on the type of problem. For example, in mechanical problems strains and stresses are of interest in addition to displacements, which are obtained after solution of the global equation system.

3.2 Software Tools Used

3.2.1 COMSOL:

1. COMSOL Multiphysics is a finite element analysis, solver and Simulation software / FEA Software package for various physics and engineering applications, especially coupled phenomena, or multiphysics. The package is platform independent. The software has several add on module which can be used to solve and simulate problems in different fields like electromagnetics, mechanics, MEMS, Chemical engineering etc. One can access the power of COMSOL Multiphysics as a standalone product through a flexible graphical user interface (GUI) or by script programming in Java or the MATLAB® language (requires the COMSOL LiveLink for MATLAB).

Using these physics interfaces, following studies can be performed:

(a) Stationary and time-dependent (transient) studies

(b) Linear and nonlinear studies

(c) Eigen frequency, modal, and frequency response studies

2. The COMSOL Desktop helps you organize simulation by presenting a clear overview of your model at any point. It uses functional form, structure, and aesthetics as the means to achieve simplicity for modeling complex realities. For instance, task-specific tools appear on the Desktop right when needed; showing only what is currently possible, which removes uncertainty from model building and brings order to simulations. The Desktop is made up of several windows, which may or may not be displayed depending on the need.

Fig 3.2. Comsol Multiphysics (Source: https://www.comsol.co.in)

3. To obtain the numerical solution or graph either matlab or excel can be used. The solution obtained for a particular parameter can be substituted in the equation for solving a particular equation or the solution can be directly plotted against the other parameter of interest like time, dimension, mode etc.

4. The RF Module solves problems in the general field of electromagnetic waves, such as RF and microwave applications, optics, and photonics. The underlying equations for electromagnetic are automatically available in all of the physics interfaces—a feature unique to COMSOL Multiphysics. This also makes nonstandard modeling easily accessible. The module is useful for component design in virtually all areas where electromagnetic waves are involved such as:

(a) Antennas

(b) Waveguides and cavity resonators in microwave engineering

(c) Optical fibers

(d) Photonic waveguides

(e) Photonic crystals

(f) Active devices in photonics

5. The physics interfaces cover the following types of electromagnetic field simulations and handle time-harmonic, time-dependent, and Eigen frequency/Eigen mode problems: •

(a) In-plane, axisymmetric, and full 3D electromagnetic wave propagation

(b) Full vector mode analysis in 2D and 3D Material properties include inhomogeneous and fully anisotropic materials, media with gains or losses, and complex-valued material properties.

6. In addition to the standard post \processing features, the module supports direct computation of S-parameters and far-field patterns. You can add ports with a wave excitation with specified power level and mode type, and add PMLs (perfectly matched layers) to simulate electromagnetic waves that propagate into an unbounded domain. For time-harmonic simulations, you can use the scattered wave or the total wave.

7. When solving the models, COMSOL Multiphysics uses the proven finite element method (FEM). The software runs the finite element analysis together with adaptive meshing (if selected) and error control using a variety of numerical solvers. The studies can make use of multiprocessor systems and cluster computing, and batch jobs and parametric sweeps can be run.

8. COMSOL Multiphysics creates sequences to record all steps that create the geometry, mesh, studies and solver settings, and visualization and results presentation. It is therefore easy to parameterize any part of the model: Simply change a node in the model tree and re-run the sequences. The program remembers and reapplies all other information and data in the model.

3.2.2 MATLAB

MATLAB (matrix laboratory) is a multi-paradigm numerical computing environment and fourth-generation programming language. A proprietary programming language developed by Math Works, MATLAB allows matrix manipulations, plotting of functions and data, implementation of algorithms, creation of user interfaces, and interfacing with programs written in other languages, including C, C++, Java, Fortran and Python.

CHAPTER 4

DESIGN AND ANALYSIS OF DIELECTRIC CYLINDRICAL NANOANTENNA

In this chapter, the design and simulations of the nanoantenna structure have been discussed. A dielectric cylindrical nanoantenna design is propose for ultra directional scattering properties. In the first section, the design of the dielectric nanoantenna and its scattering properties has been discussed in detail. In the next section a design of tunable cylindrical dielectric nanoantenna by varying nanocylinder parameters has been demonstrated.

4.1 Motivation and design approach

The unavoidable problems of metallic structures like high intrinsic losses motivated the study of high-dielectric nanoantenna structures [64]. Interestingly, dielectric nanoantennas present sharp resonances and have low dissipative losses in visible and near-infrared regions. High all-dielectric nanoparticles can support both electric and magnetic resonances, which can be controlled independently. It has been observed in previous studies that efficient response can be achieved when nanoparticles possess both electric and magnetic resonances. These interesting advantages over metallic counterparts make dielectric nanoantennas as popular choices for directional scattering in visible and near-infrared regions.

It is evident from past studies that the effective engineering of scattering radiation depends on the electric and magnetic responses to the incident electromagnetic wave in dielectric nanoparticles. The unusual electromagnetic scattering effects on magnetodielectric particles were first theoretically proposed by Kerker et al [65]. The scattering radiation of magnetodielectric particles exhibiting both electric and magnetic resonances can be controlled under certain conditions for the values of electric permittivity ε and magnetic permeability μ, as given by Kerker et al. According to Kerker, due to the interference of magnetic and electric dipolar resonances, the complete forward or backward scattering is possible. The prediction by Kerker et al. has given new direction in the field of optical nanoantennas. At zero-backward intensity

condition or Kerker's first condition, the scattered field is mainly in direction of the incoming wave, with zero backward scattering which leads to interesting nanoantenna applications.

According to Mie theory the first and second lowest resonances of dielectric spherical nanoparticles indicates the magnetic and electric dipole terms respectively [66]. For high permittivity particles, the quality factor of Mie resonances increases resulting in high scattering efficiency. In literature, the theoretical and experimental demonstrations of strong electric and magnetic dipolar resonances of high-dielectric spherical particles like Si or Ge in the visible and near infrared regions have been reported based on Mie theory [67-70]. It has been shown that it is possible to tune electric and magnetic resonance at a particular frequency for Silicon nanoparticles by changing their shape and size [71, 72]. The enhancement of light absorption by periodic Silicon cylindrical nanopillars has been also demonstrated [73].

Here, we propose the design of cylindrical nanoantennas, using scattering properties of nanocylinders by applying Kerker's condition for unidirectional forward scattering. We theoretically investigate and numerically demonstrate the scattering properties of dielectric nanocylinders. The ability of dielectric nanocylinders to control light scattering in desired direction efficiently makes them promising candidates for low loss, tunable and ultra-directional nanoantenna applications. The scattering by Ge nanocylinder homodimers has been demonstrated. Next, an array of Ge nanocylinders for highly directive nanoantenna application has been demonstrated. The effect of number of array elements on directivity of nanoantenna has been also studied. All numerical results are obtained using the finite element method (FEM) explained in chapter 2.

4.2 Design Parameters and scattering analysis of Ge nanocylinder

Design: A dielectric Ge nanocylinder of radius $r = 50\,nm$ and height $h = 150\,nm$ has been considered as shown in figure 4.1. The optical properties of the material have been taken from reference [74]. The nanocylinder dimensions are chosen such that the operating wavelength falls in visible region. The operating wavelength can be tuned at desired wavelength by changing the dimensions of nanocylinder. For simulation of cylindrical nanoparticle a space was designed with dielectric nanoantenna at the origin being suspended in air.

A PML (perfectly matched layer) layer was created to completely surround the entire simulation space which will absorb scattered light in all direction.

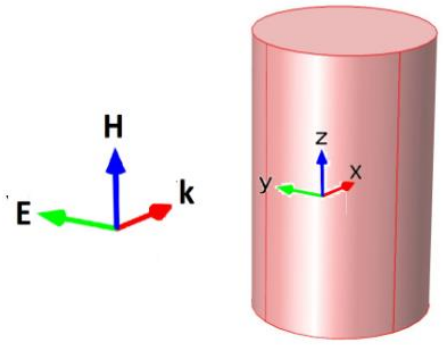

Fig. 4.1 Schematic of a Ge nanocylinder

Scattering Analysis: The nonmagnetic nanoparticle is characterized by the electric current density *J* and polarization *P*. The electric current density and polarization induced by external electromagnetic fields are related by $J = -i\omega P$, where ω is the angular frequency [75, 76]. The relative magnetic permeability μ of the particle in nonabsorbent medium is given by μ =1.The time average extinction power P_{ext} ($P_{ext} = P_{sca}$) for electromagnetic scattering in non-absorbing nonmagnetic medium is given by

$$P_{ext} = \frac{\omega}{2} Im \int E_0^*(r).P(r)dV' \qquad (4.1)$$

where, $E_0^*(r)$ denotes the electric field of the incident electromagnetic waves, V' is the volume of the scattering object and *r* denotes the position coordinate. *P(r)* is denotes the position coordinate. *P(r)* is defined as

$$P(r) = \varepsilon_0(\varepsilon_r - 1)E(r) \qquad (4.2)$$

where ε_0,ε_r denotes the permittivity of free space and relative permittivity of the nanoparticle respectively. *E(r)* is the total electric field which is equal to the sum of incident electric field and scattered electric field.

From multipole decomposition of scattering power we get,

$$p_{sca} \approx {p^p}_{sca} + {p^m}_{sca} + {p^Q}_{sca} + {p^M}_{sca} + \cdots \qquad (4.3)$$

where, ${p^p}_{sca}$ is scattering power for electric dipole, ${p^m}_{sca}$ is scattering power for magnetic dipole and ${p^Q}_{sca}$, ${p^M}_{sca}$ are scattering powers for electric and magnetic quadrupoles respectively.
The total scattering power can be written as

$$p_{sca} = \frac{c^2 {k_0}^4 Z_0}{12\pi}|p|^2 + \frac{c^2 {k_0}^4 Z_0}{12\pi}|m|^2 + \frac{c^2 {k_0}^6 Z_0}{40\pi}\sum\left|Q_{\alpha'\beta'}\right|^2 + \frac{c^2 {k_0}^6 Z_0}{160\pi}\sum\left|M_{\alpha'\beta'}\right|^2 + \ldots \quad (4.4)$$

where, p is the electric dipole moment, m is the magnetic dipole moment, Q is electric quadrupole tensor and M is the magnetic quadrupole tensor. Scattering powers at higher order modes are negligible so we can neglect the higher order modes in calculations.

$$p = \varepsilon_0(1-\varepsilon_r)\int_v E(r')dV' \quad (4.5)$$

$$m = \frac{i\omega\varepsilon_0(1-\varepsilon_r)}{2c}\int_v [r \times E(r')]dV' \quad (4.6)$$

where, c is the speed of light in vacuum, $k_0 = \frac{\omega}{c}$ represents free space wave number, $z_0 = \frac{1}{\varepsilon_0 c}$ is free space impedance, and $\alpha', \beta' = x, y, z$ denote Cartesian components [77]
From the Eq. (4)-(6) the scattering cross section (σ_{sca}) associated to each multipole can be calculated by simply normalizing each scatter power by the incident power density (I_0), given by

$${\sigma^p}_{sca} = \langle p_{sca,ED}\rangle / I_0 \quad (4.7a)$$

$${\sigma^m}_{sca} = \langle p_{sca,MD}\rangle / I_0 \quad (4.7b)$$

The scattering spectrum of Ge nanocylinder has been obtained as shown in figure 4.2(a). The scattering spectrum peaks, denote the modes at corresponding wavelengths i.e. the electric resonance at $\lambda = 482$ nm and magnetic resonance at $\lambda = 550$ nm. Figure 4.2(b) depicts the 2D normalized polarization distribution at magnetic and electric dipole resonances. At electric and magnetic dipolar resonance peaks, the scattering radiation pattern is symmetrically distributed in both forward and backward directions. However, the unidirectional scattering can be obtained in the presence of electric and magnetic interferences.

The direction of scattering radiation is determined according to the polarity of Re ($\alpha_e \alpha^*_m$), whether positive or negative.

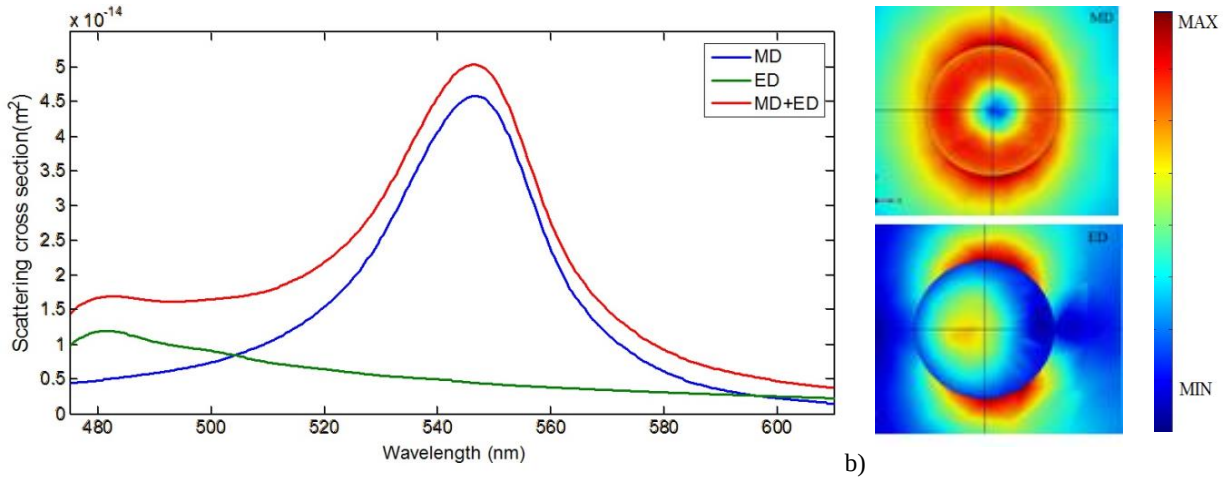

Fig. 4.2 Scattering analysis for Germanium nanocylinder. (a) Scattering cross-section of the electric (ED), magnetic dipoles (MD) and total scattering cross-section. (b) Normalized 2D polarization distribution patterns for MD at $\lambda = 550$ nm and ED at $\lambda = 482$ nm.

The positive value of Re $(\alpha_e \alpha^*{}_m)$ indicates forward scattering, where α_e and α_m are the electric and magnetic complex scalar polarizability of the nanoparticle respectively, is given by

$$\alpha_e \equiv \frac{p_x}{(\varepsilon_0 |E_0|)} \qquad (4.8a)$$

$$\alpha_m \equiv \frac{m_y}{(|H_0|)} \qquad (4.8b)$$

where, E_0 and H_0 are the electric and magnetic field of the incident plane wave respectively.

Unidirectional Forward scattering with complete suppression of backward scattering can be achieved when the interference between electric and magnetic dipoles satisfy the first generalized Kerker's condition,

$$\frac{\alpha_e}{\varepsilon_s} = \mu_s \alpha_m \;\; ; \;\; \frac{d\sigma_{sca}}{d\Omega}(180^0) = 0 \qquad (4.9)$$

with ε_s and μ_s being the relative permittivity and permeability of the surrounding medium respectively.

Further, the variation of electric and magnetic polarizabilities with respect to wavelength has been obtained as shown in figure 4.3. At $\lambda = 595$ nm, the first GK condition is satisfied that is $\alpha_e = \alpha_m$, indicated by point of intersection of electric and magnetic polarizability in figure 4.3(a).

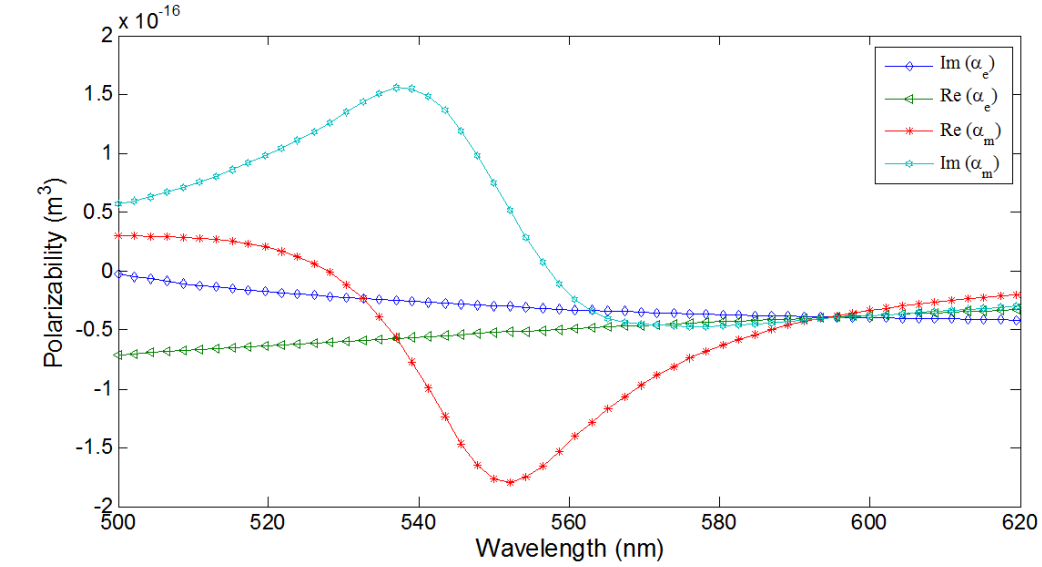

a)

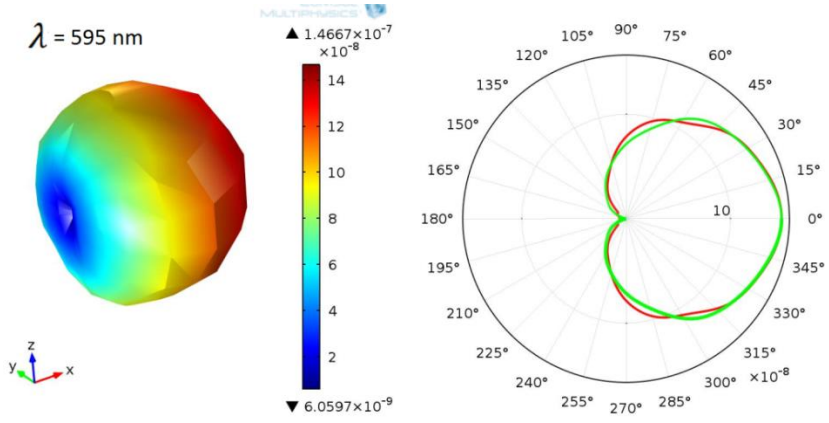

b)

Fig. 4.3. Variation of electric and magnetic polarizabilities with respect to wavelength. a) Spectra showing variation of polarizabilities. At $\lambda = 595$ nm the first forward scattering condition is satisfied with zero backscattering. b) 3D and 2D far-field pattern obtain at $\lambda = 595$ nm.

3D and 2D far field patterns shown in figure 4.3(b) exhibit the total forward scattering with complete suppression of backward scattering at $\lambda = 595$ nm. The observed scattering pattern exhibits complete azimutal symmetry. Thus, high permittivity nanocylinders can be used for unidirectional nanoantenna applications.

4.3 Scattering pattern of cylindrical nanoantenna homodimers

Two identical Ge nanocylinders of radius $r = 50$ nm and height $h = 150$ nm with spacing $d = 200$ nm has been considered as shown in figure 4.4(a). The far-field pattern of homodimers has been observed at $\lambda = 595$ nm as shown in figure 4.4(b).

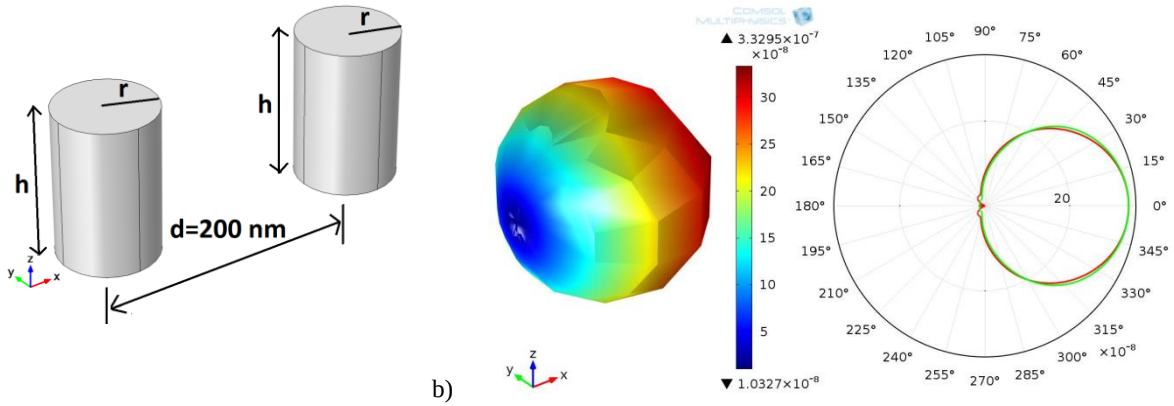

Fig. 4.4 (a) Schematic of Ge nanocylinder homodimers of radius $r = 50$ nmand $h = 150$ nm. (b) 3D and 2D normalized far-field patterns at $\lambda = 595$ nm.

The far-field pattern obtained for homodimers with $d = 200$ nm gets enhanced as compared to the far-field pattern for single nanocylinder which results from the constructive interferences of far-fields of two individual nanocylinders. Complete forward scattering in direction $\theta = 0°$ has been observed. It has been observed that cylindrical homodimers offer better directionality over individual cylindrical nanoantenna. Further, the far-field patterns have been obtained by varying the spacing between nanocylinder homodimers as shown in figure 4.5(a)-4.5(f). The effect of d on scattering pattern has been demonstrated by comparing three cases: $d < \lambda/2$, $d > \lambda/2$ and $d > \lambda$.

In the first case where d has been kept as $d < \lambda/2$ ($d = 200$ nm), one major is observed as shown in figure 4.5(a) and 4.5(d). In the second case, where $d > \lambda/2$ ($d = 350$ nm), the directivity is further increased as compared to directivity of homodimers in case of d less than $\lambda/2$. As d increases the phase delay between cylindrical homodimers lead to collective grating diffractions. The phase delay between homodimers is given by $\Delta\varphi = kd\,(\cos\theta - 1)$=0 where, $k = 2\pi/\lambda$.

$d < \lambda/2$	$d > \lambda/2$	$d > \lambda$

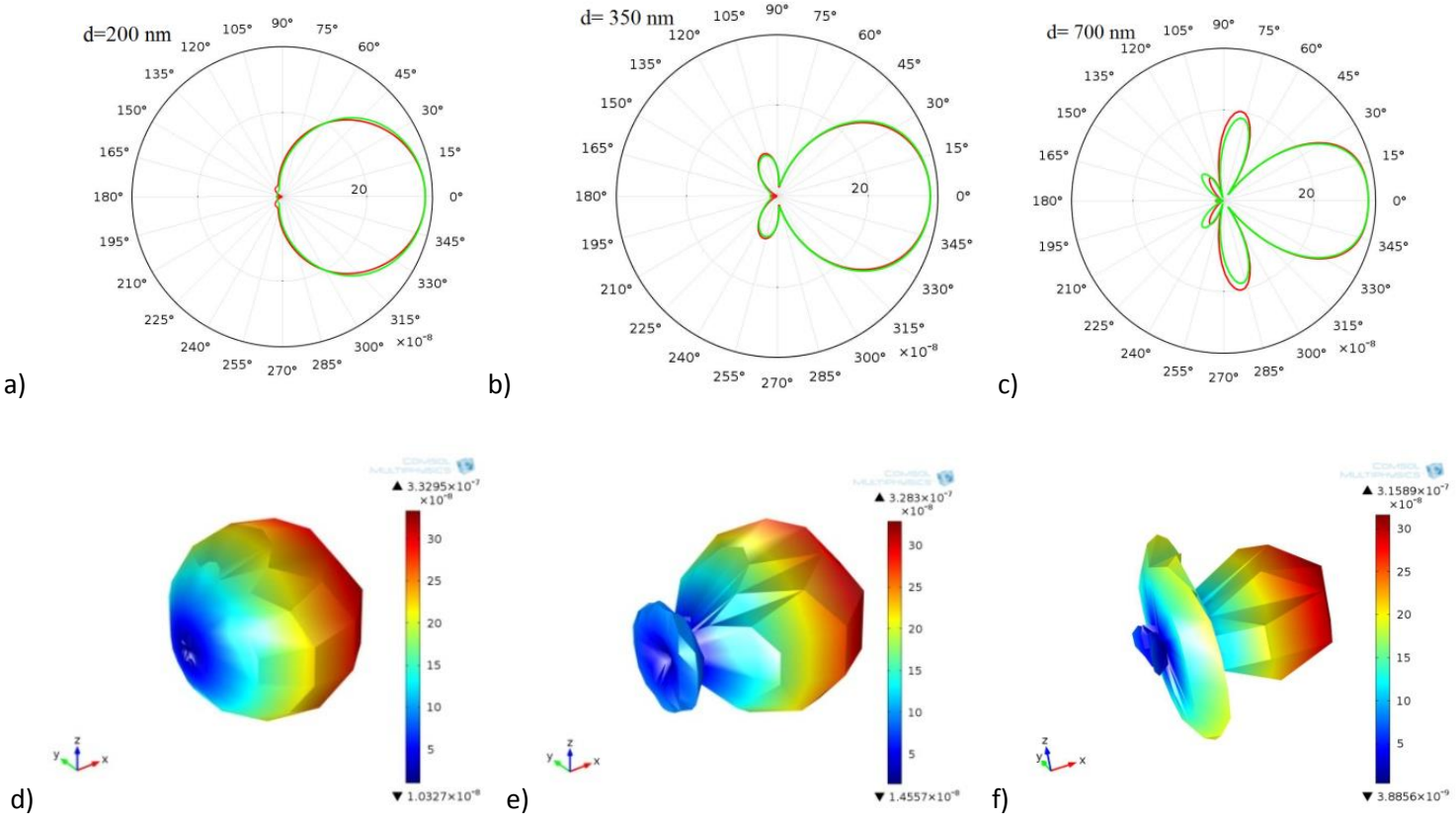

Fig. 4.5 Far-field patterns showing the effect of spacing d on directionality of nanocylinder homodimers. 2D and 3D far-field patterns when $d < \lambda/2$ [(a) and (d)], $d > \lambda/2$ [(b) and (e)] and $d > \lambda$ [(c) and (f)].

Next, for $d > \lambda$ ($d = 700$ nm) directivity increases but the scattering strength further decreases One major lobe with four side lobes at $81.4°, 134.4°, 225.6°$ and $278.6°$ have been observed as shown in figure 4.5(c) and 4.5(f).

For higher order diffractions, the diffraction angles can be calculated at using formula given by $\beta_m = \arccos(1 - m\lambda/d)$[78] where m is order of the diffraction which is same as obtained from above far-field pattern. It has been observed that the directivity of the homodimers increases with increase in d but as d increases the diffraction grating effect becomes dominant leading to the increase in the number of side lobes. The diffraction grating effect results in scattering undesired directions which further reduces the scattering strength of main lobe.

4.4 Linear array of cylindrical nanoantenna

As observed that the directionality is enhanced by using a pair of cylindrical nanoantennas. To further enhance the directivity, an array of Ge cylindrical nanoparticles has been deployed. An array of Ge nanocylinders of radius=50 nm and height=150 nm with spacing $d = 250$ nm ($d < \lambda/2$) so as to avoid diffraction grating effect has been considered for forward scattering at wavelength 595 nm.

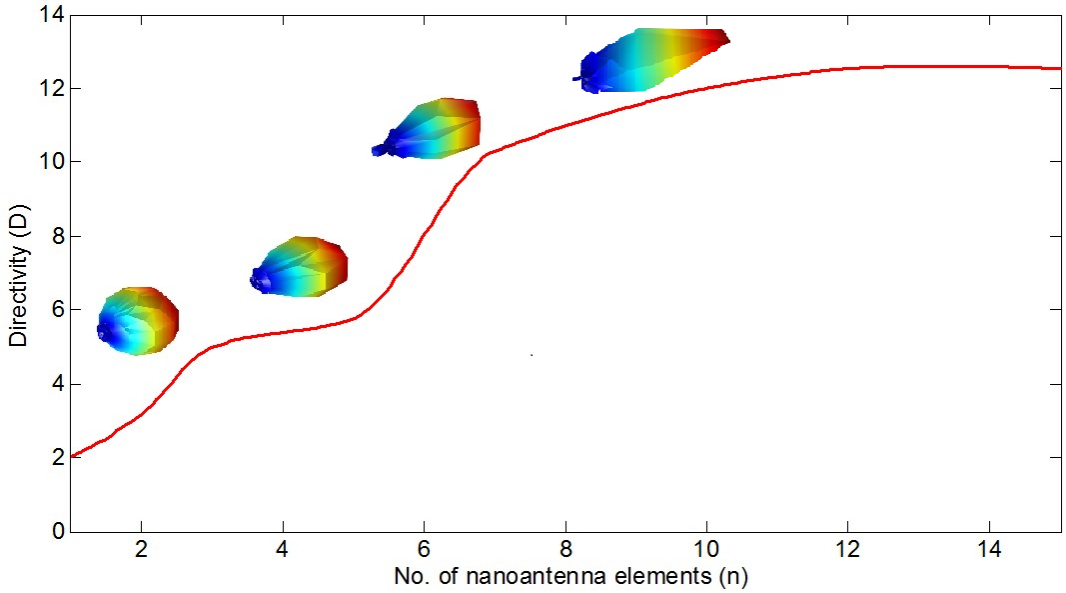

Fig. 4.6 Variation of directivity with respect to number of nanoantenna array elements.

The directivity and far-field pattern of the linear array of cylindrical nanoantenna with varying number of elements in the array has been obtained as shown in figure 4.6. It has been observed that the directivity increases with respect to increase in the number of array elements. However, for a value of $n > 10$ no further significant improvement in directivity of nanoantenna is observed.

4.5 Conclusion

In this section, the unidirectional scattering by Ge nanocylinders has been demonstrated. The Kerker's type, forward scattering in visible region at wavelength 595 nm for Ge nanocylinders has been demonstrated. The scattering by Ge nanocylinder homodimers have been analyzed by varying the spacing between nanocylinders. It has been observed that as gap increases the

directivity increases but as gap exceeds $\lambda/2$ the diffraction grating effect becomes dominant which results in scattering in undesired directions. Due to scattering in undesired directions the strength of scattering in desired direction gets reduced. Thus, for nanocylinder array the gap between nanoantenna elements must not exceed $\lambda/2$ to avoid diffraction grating effects. Next, for highly directive forward scattering applications a linear chain of nanoantenna array has been demonstrated. It has been demonstrated that with increase in the number of nanoantenna elements in an array the directionality increases however, after a limit the increase in directivity is not significant.

CHAPTER 5

EFFECT OF NANOCYLINDER PARAMETERS AND MATERIALS ON SACTTERING PROPERTIES

5.1 Overview

The scattering properties of a nanoparticle are strongly dependent on the particle design parameters and dielectric material used. In this chapter, the effect of both the nanoparticle design parameter and dielectric material on the scattering properties of all-dielectric nanocylinder is discussed in detail. A dielectric nanocylinder identical to the one designed in chapter 4 is considered. It is clear from discussion in chapter 4 that a dielectric nanocylinder behaves as a nanoantenna in visible and near infrared region. In this section first, the effect of dielectric materials used for design of nanocylinder on its electric and magnetic dipole resonances is studied. The scattering properties of nanocylinders of different dielectric materials Ge, Si and AlAs have been compared. The dielectric constant of material is further reduced to observe its influence on the nanocylinder. Next, nanocylinder parameters are changed i.e. radius and height, to observed the change in nanoantenna properties.

5.2 Effect of nanocylinder material on scattering properties

5.2.1 Design approach

A dielectric nanocylinder of $h = 150$ nm and $r = 50$ nm considered. For a comparison, we first demonstrate the scattering spectra for cylindrical nanoantennas of three different dielectric materials. Scattering cross-section for electric and magnetic dipoles are calculated based on FEM simulations. Design of simulation space and PML is same as that for nanocylinder in chapter 4.

5.2.2 Simulations and results

To analyze the influence of nanocylinder material on scattering properties, the scattering spectrum for nanocylinder of different materials (Ge, Si, AlAs) are demonstrated. The scattering spectra observed for all materials are shown in figure 5.1.

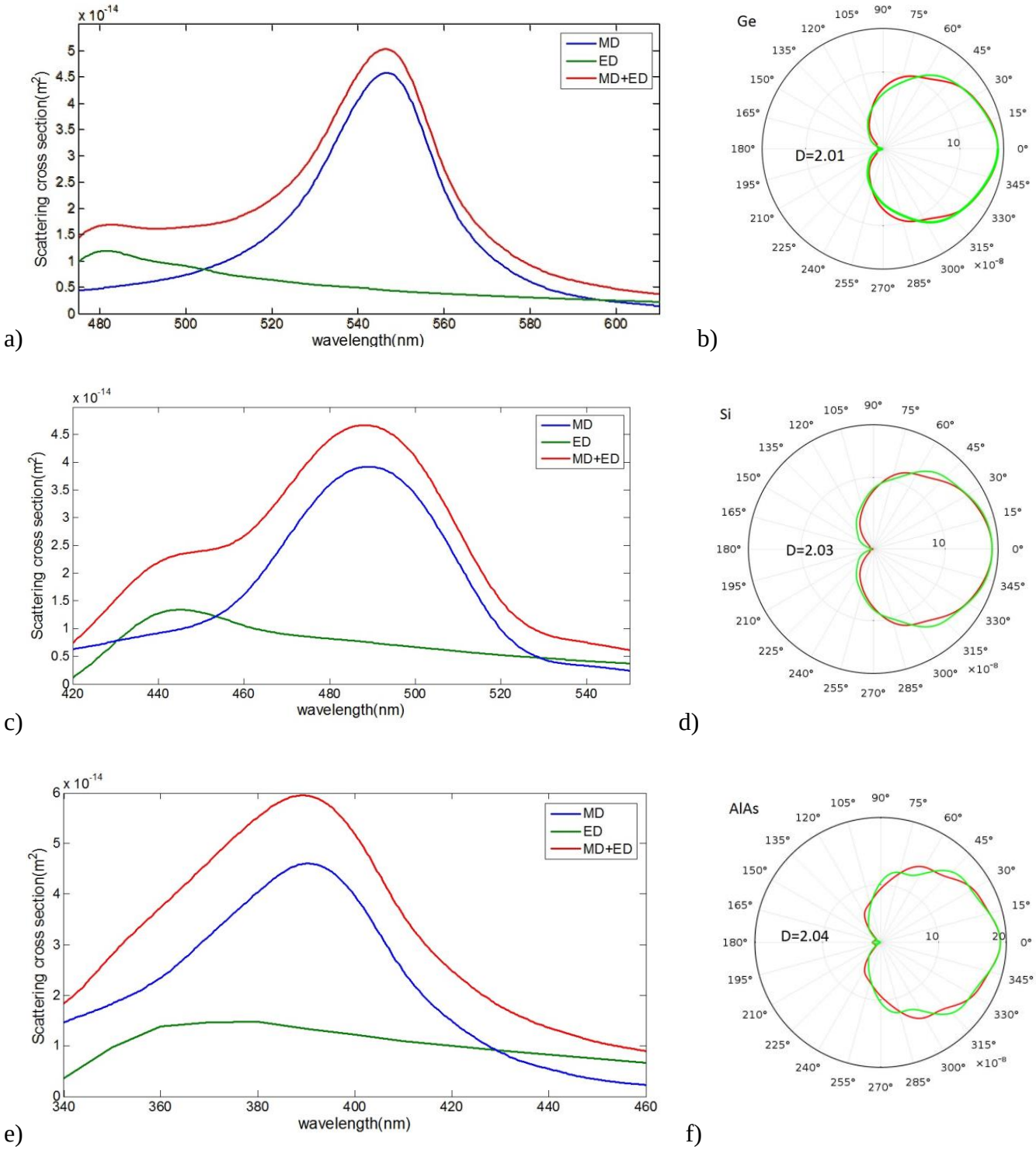

Fig. 5.1 Scattering spectra for nanocylinder of different materials. Scattering cross-section for electric and magnetic dipolar resonances for Ge, Si, AlAs [(a), (c) and (e)]. Far-filed patterns at first GK condition [(b), (d) and (f)].

Electric and magnetic resonances for Ge nanocylinder are observed at $\lambda = 482$ nm and $\lambda = 550$ nm (figure 5.1(a)). Si nanocylinders have electric and magnetic resonances at $\lambda = 445$ nm and $\lambda = 491$ nm as shown in figure 5.1(c). Similarly, AlAs nanocylinders (figure 5.1(e)) poses electric and magnetic responses at $\lambda = 363$ nm and $\lambda = 392$ nm. It is observed that as permittivity of dielectric material decreases the gap between electric and magnetic dipolar resonances decrease and vice-versa.

We further observed the far-field patterns of all nanocylinders at wavelengths where first GK condition is satisfied. From the far-field patterns (as shown in figure 5.1(b, d and f)) at first GK condition we observe complete forward scattering with zero backward scattering. It is also found that as permittivity of dielectric material increase the directivity starts decreasing where as for material of lower permittivity we observe slight increase in directivity. Hence by changing the material we can also tune the electric and magnetic resonances of cylindrical nanoantenna.

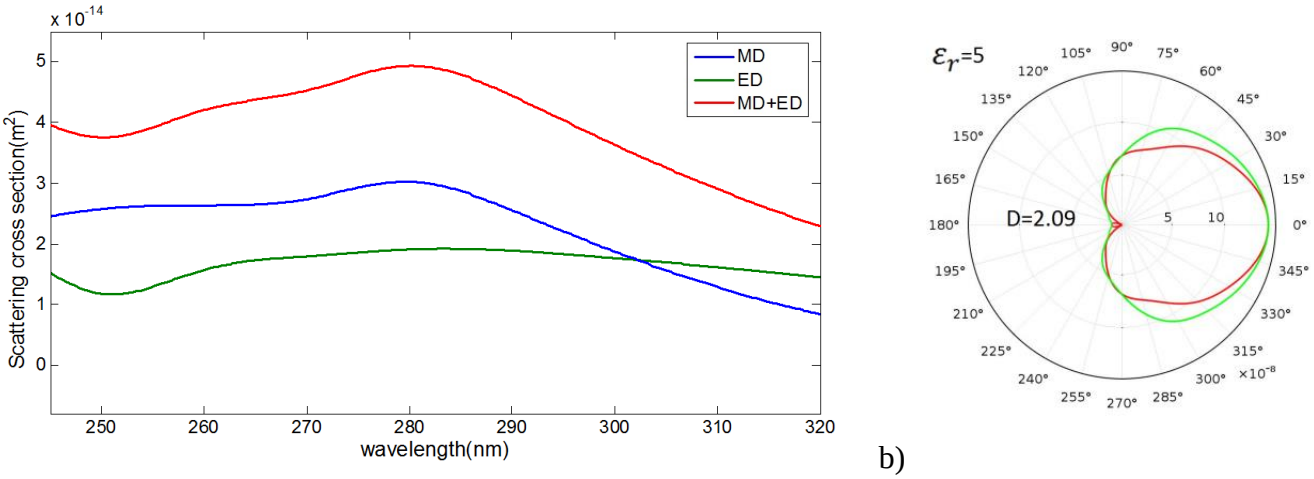

a) b)

Fig. 5.2 Scattering spectra (a) and far-field pattern (b) at first GK condition for cylindrical nanoantenna of permittivity $\varepsilon_r = 5$.

We further study the effect of scattering properties for much lower permittivity, lower than AlAs. To study the scattering properties of cylindrical nanoantenna for much lower permittivity we have demonstrated the scattering by nanocylinder of same dimension having ε_r=5. Scattering spectra obtained from FEM simulations is shown in figure 5.2(a). We observed that as permittivity decreases electric and magnetic resonance shifts towards each other. The electric and magnetic resonant modes at $\lambda = 264$ nm and $\lambda = 281$ nm nearly merge with each other.

5.2.3 Conclusion

From the above analysis of nanocylinders of different materials we conclude that the electric and magnetic resonant mode shift depending on the value of permittivity. For higher values of permittivity, gap between electric and magnetic resonant modes is larger whereas for lower permittivity materials resonant modes nearly merge with each other. We observed that with decrease in gap between dipolar resonances the strength of interference between electric and magnetic resonances gets increased, resulting in more directive scattering radiation.

5.3 Influence of nanocylinder parameters on scattering properties

5.3.1 Design approach

In this section we have discussed the detail analysis of the effect of the variation in the nanocylinder parameters on scattering properties and directionality of the cylindrical nanoantenna. A Ge nanocylinder identical to the one used in above section has been considered for this purpose. The radius and height of the nanocylinder are varied to study the influence on the scattering properties. Further, the change in directivity of the nanoantenna for different parameters was observed. Further influence of increase in diameter of nanocylinder on electric and magnetic dipolar interference has been studied. Forward and backward scattering at first and second GK condition have been analyzed for nanoantenna applications. For this purpose we have consider the identical nanocylinder discussed above (in section 5.1).

5.3.2 Simulations and results

The scattering spectra of the Ge cylinders of different radius keeping the height constant are observed. For, $r = 50$ nm and $h = 150$ nm the scattering spectra is shown in figure 5.1(a) with electric resonance at $\lambda = 482$ nm and magnetic resonance at $\lambda = 550$ nm. When we increase the radius of nanocylinder r= 60 nm, the electric and magnetic resonances are observed at wavelengths $\lambda = 528$ nm and $\lambda = 639$ nm, respectively as shown in figure 5.3.

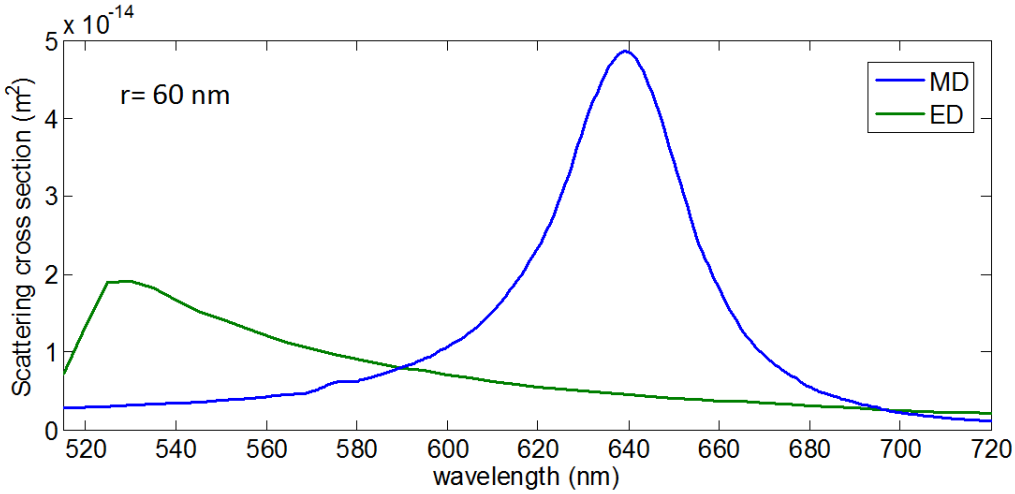

Fig. 5.3 The scattering spectrum for Ge cylinder of radius $r = 60$ nm and height $h = 150$ nm.

Further increasing the radius to $r = 65$ nm, the electric and magnetic dipole resonance are observed at $\lambda = 550$ nm and $\lambda = 680$ nm, respectively as shown in figure 5.4.

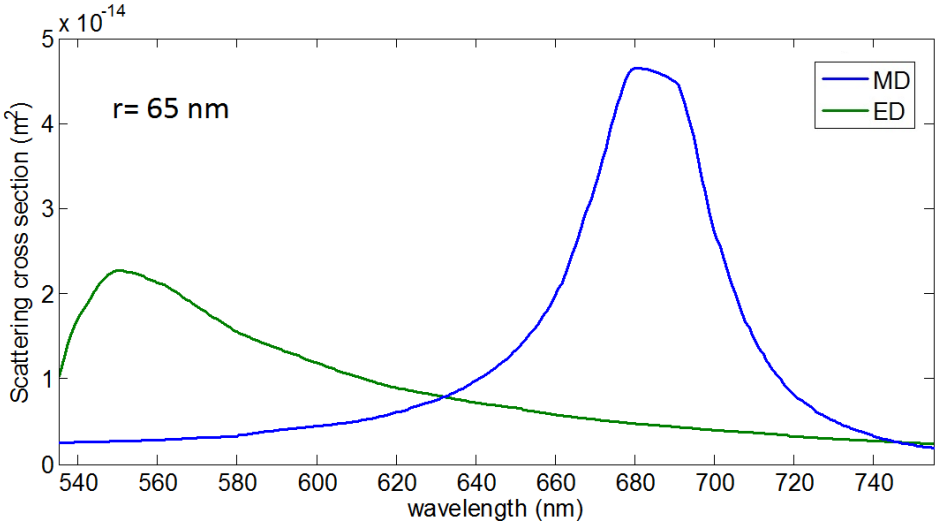

Fig. 5.4 The scattering spectrum for Ge cylinder of radius $r = 60$ nm and height $h = 150$ nm.

From above observations it is clear that the scattering properties changes with change in radius of the nanocylinder. It is observed that with increase in the radius of the nanocylinder the wavelength of electric and magnetic resonances shift towards left i.e. blue shift. However, there is no significant change in scattering cross section.

Next, to study the effect of change in nanocylinder height on scattering properties we kept the radius constant $r = 50$ nm and varied the height of nanocylinder.

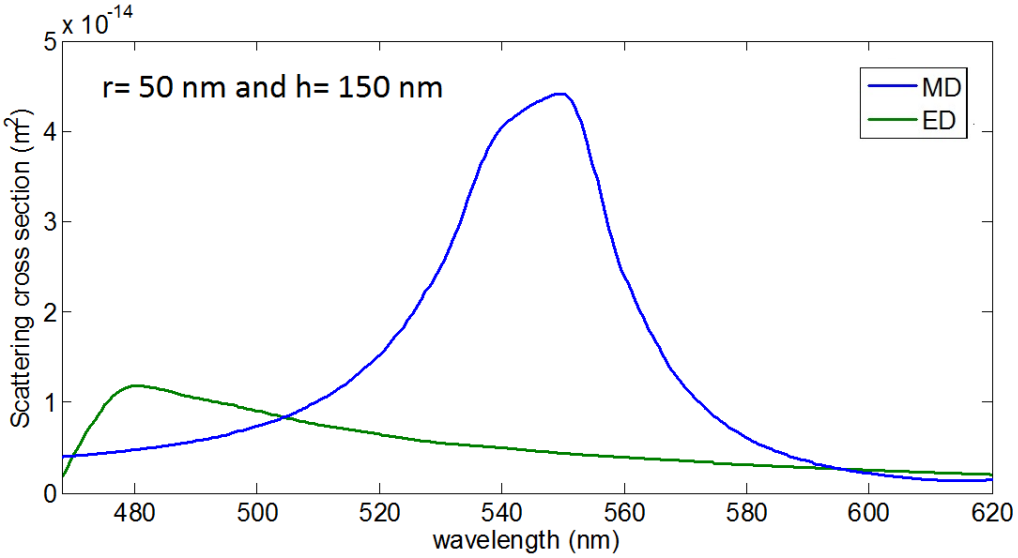

Fig. 5.5 The scattering spectrum for Ge nanocylinder of $r = 50$ nm and $h = 150$ nm.

First the scattering spectrum for nanocylinder of $r = 50$ nm and $h = 150$ nm is observed as shown in figure 5.5. The height of the nanocylinder is increased i.e. $h = 160$ nm keeping the radius constant. The scattering spectrum is observed as shown in figure 5.6.

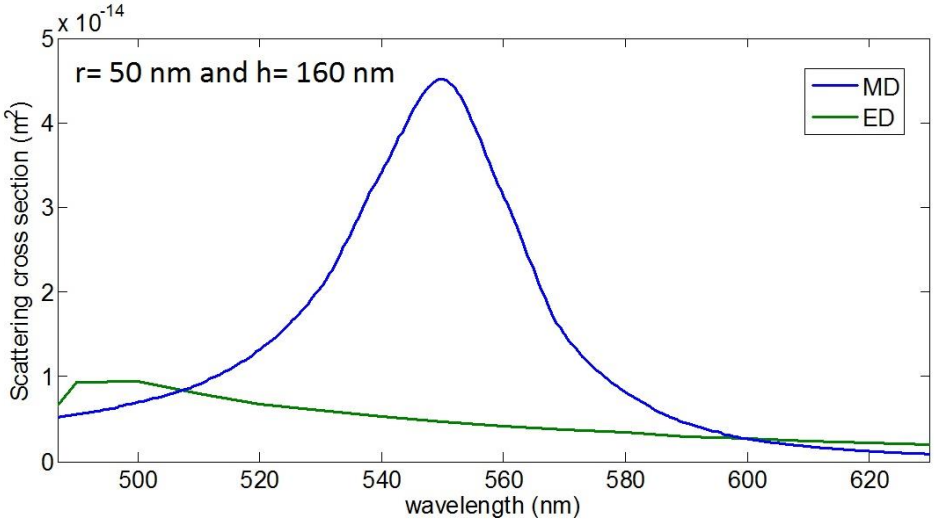

Fig. 5.6 The scattering spectrum for Ge nanocylinder of $r = 50$ nm and $h = 160$ nm.

We observed that there is no significant influence of nanocylinder height on the scattering property. The scattering spectrums for different height of nanocylinder are almost same that is there is no shift in electric and magnetic dipole resonance wavelengths.

5.3.3 Conclusion

From above observations we can conclude that the scattering properties of the nanocylinder are highly dependent on its radius. As we increase the radius of the nanocylinder the electric and magnetic resonances shift towards right. This has great importance on the tunablity of the nanoantenna. A nanoantenna can be tune to a particular wavelength by varying the radius of nanocylinder. However, with increase in the height of the nanocylinder no significant change in scattering properties of the nanoantenna is observed. Hence, nanocylinder can be used for designing the nanorods or nanowires as its scattering properties do not change with the variation in height.

CHAPTER 6

CONCLUSION AND FUTURE SCOPE

6.1 Conclusion

In this dissertation, scattering by a dielectric nanocylinder has been demonstrated for nanoantenna applications in visible and near infrared region. It has been observed that for efficient scattering of light can be achieved by an array of nanocylinders keeping the space between nanoelements less than $\lambda/2$ to avoid diffraction grating effects. For highly directive applications we can increase the directivity by increasing the number of nanoantenna elements in an array. However, after a certain limit there will be no significant increase in the directivity.

Further, the effect of the dielectric permittivity of the nanocylinder on the scattering properties has been observed. It has been observed that as dielectric permittivity of the nanocylinder is increased the gap between electric and magnetic resonant modes increases. However, as the dielectric permittivity decreases the gap between the resonance modes decreases and the strength of the interference increases which results in high directivity of the nanoantenna. The radius of nanocylinder has great influence on the scattering properties. The electric and magnetic resonances of the nanocylinder shift towards right with increase in radius. Hence the scattering of an all-dielectric cylindrical antenna can be tune by tuning the radius for a desired wavelength. It has been observed that scattering properties of the nanocylinder does not change with change in height. This property has great advantages in design of nanorods and nanowires.

6.2 Future scope

The research in field of all-dielectric nanoantennas has great scope in the field of nanophotonics. In this thesis, we have highlighted the ultra-directional scattering by all- dielectric cylindrical nanoantennas invisible region. As we have seen, the purposed design of dielectric nanoantennas can be tuned for any wavelength by controlling the radius of nanocylinder. This property can be used to design new dielectric cylindrical nanoantennas for desired application range. Another property of dielectric cylindrical nanoantennas is dependence of interference strength of electric and magnetic resonances on the dielectric permittivity of the material. Hence, strength of

interferences can be controlled by using appropriate dielectric material. The all-dielectric cylindrical nanoantennas can be used for design of optical nanowires in visible and near-infrared regions as its scattering properties remain unchanged with increase in height.

REFERENCES

[1] L. Novotny and B. Hecht, *Principles of Nano-Optics*, Cambridge University Press, 2012.

[2] M. W. Knight, H. Sobhani, P. Nordlander, and N. J. Halas, "Photodetection with active optical antennas", Science 332,702–704, (2011).

[3] L. Novotny and N. Van Hulst, "Antennas for light", Nat. Photonics 5, 83–90 (2011).

[4] H. A. Atwater and A. Polman, "Plasmonics for improved photovoltaic devices", Nat. Mater. 9, 205–213 (2010).

[5] D. Sikdar, I. D. Rukhlenko, W. Cheng, and M. Premaratne, "Optimized gold nanoshell ensembles for biomedical applications", Nanoscale Res. Lett. 8, 142–146 (2013).

[6] M. F. Garcia-Parajo, "Optical antennas focus in on biology", Nature Photonics 2, 201–203 (2008).

[7] B. J. Roxworthy, K. D. Ko, A. Kumar, K. H. Fung, E. K. C. Chow, G. L. Liu, N. X. Fang, and K. C. Toussaint, "Application of plasmonic bowtie nanoantenna arrays for optical trapping, stacking, and sorting", Nano Lett. 12, 796–801(2012).

[8] John Wessel, "Surface-enhanced optical microscopy," J. Opt. Soc. Am. B 2, 1538-1541 (1985)

[9] L. Rosa, K. Sun and S. Juodkazis, "Sierpin´ski fractal plasmonic nanoantennas", Phys. Status Solidi RRL 5, 175 (2011)

[10] A. Alu and N. Engheta, "Herzian plasmonic nanodimmer as an efficient nanoantenna," Phys. Rev. B 78 (19), 195111 (2008).

[11] A. E. Krasnok, A. E. Miroshnichenko, P. A. Belov, and Yu. S. Kivshar, "Huygens optical elements and Yagi-Uda nanoantennas based on dielectric nanoparticles," JETP Letters 94, 635-640 (2011).

[12] M. Kerker, D. S. Wang, and C. L. Giles, "Electromagnetic scattering by magnetic spheres," J. Opt. Soc. Am. 73, 765–767 (1983).

[13] A. E. Krasnok, A. E. Miroshnichenko, P. A. Belov, and Y. S. Kivshar, "All-dielectric optical nanoantennas," Opt. Express 20, 20599–20604 (2012).

[14] C. A. Balanis, *Antenna theory: analysis and design*, John Wiley and Sons, New York, 2nd edition,1997.

[15] A. E. Krasnok , I. S. Maksymov , A. I. Denisyuk , P. A. Belov , A. E. Miroshnichenko, C. R. Simovskii and Y. S. Kivshar , "Optical nanoantennas" ,Phys. Usp. 56, 539–564 (2013).

[16] M. I. Stockman, “Nanoplasmonics: past, present, and glimpse into future", Optics Express 19, 22029 (2011).

[17] J. D. Jackson , “Classical electrodynamics", John Wiley Sons, 2006.

[18] V. Giannini, A. I. Fernández-Domínguez, , Y. Sonnefraud, T. Roschuk, R. Fernández-García, and S. A. Maier, “Controlling Light Localization and Light–Matter Interactions with Nanoplasmonics”, Small 6, 2498–2507 (2010).

[19] P. Bharadwaj, B. Deutsch, and L. Novotny, “Optical Antennas," Advances in Optics and Photonics 1, 438 (2009).

[20] J. A. Schuller, E. S. Barnard, W. Cai, Y. C. Jun, J. S. White, and M. L. Brongersma, “Plasmonics for extreme light concentration and manipulation", Nature Materials 9,193-204 (2010).

[21] J. N. Farahani, H.J. Eisler, D. W. Pohl, M. Pavius, P. Fluckiger, P. Gasser, and B. Hecht, “Bow-tie optical antenna probes for single-emitter scanning near-field optical microscopy", Nanotechnology 18, 125506 (2007).

[22] T. H. Taminiau, R. J. Moerland, F. B. Segerink, L. Kuipers, and N. F. van Hulst, “$\lambda/4$ resonance of an optical monopole antenna probed by single molecule uorescence", Nano Letters 7, 28-33 (2007)

[23] F. De Angelis, M. Patrini, G. Das, I. Maksymov, M. Galli, L. Businaro, L.C. Andreani, E. Di Fabrizio, **“**A hybrid plasmonic-photonic nanodevice for label-free detection of a few molecules”, Nano Letters 8, 2321 (2008).

[24] A. W. Bargioni, A. Schwartzberg, M. Cornaglia, A. Ismach, J. J. Urban, Y. J. Pang, R. Gordon, J. Bokor, M. B. Salmeron, D. F. Ogletree, P. Ashby, S. Cabrini, and P. J. Schuck, “Hyperspectral Nanoscale Imaging on Dielectric Substrates with Coaxial Optical Antenna Scan Probes”, *Nano Letters 11*, 1201-1207 (**2011**).

[25] A. N. Kolerov, “Near-field scanning microscope with carbon nanotube probe”, Technical Physics Letters 37, 259 (2011).

[26] Kneipp K, Moskovits M, Kneipp H (Eds), *Surface-Enhanced RamanScattering: Physics and Applications*, Springer, Berlin, 2006.

[27] Moskovits M, “Surface-enhanced spectroscopy”, Rev. Mod. Phys. 57, 783--826 (1985).

[28] A. Brolo, E. Arctander, R. Gordon, B. Leathem, and K. Kavanagh, “Nanohole-Enhanced Raman Scattering,” Nano Lett. 4(10), 2015–2018 (2004).

[29] J. J. Baumberg, T. A. Kelf, Y. Sugawara, S. Cintra, M. E. Abdelsalam, P. N. Bartlett, A. E. Russell, "Angle-Resolved Surface-Enhanced Raman Scattering on Metallic Nanostructured Plasmonic Crystals", Nano Lett. 5, 2262−2267 (2005).

[30] N. Anderson, A. Hartschuh, and L. Novotny, "Chirality changes in carbon nanotubes studied with near-field raman spectroscopy", Nano Letters 7, 577-582 (2007).

[31] L. G. Canado, A. Hartschuh, and L. Novotny, "Tip-enhanced raman spectroscopy of carbon nanotubes", Journal of Raman Spectroscopy 40, 1420-1426 (2009).

[32] H. Nalwa, *Handbook of thin film materials: Deposition and processing of thin films*, Academic Pr, vol. 5, 2002.

[33] A. Sundaramurthy, P. J. Schuck, N. R. Conley, D. P. Fromm, G. S. Kino, and W. E. Moerner, "Toward nanometer-scale optical photolithography: utilizing the near-field of bowtie optical nanoantennas", Nano Letters 6, 355-360 (2006).

[34] Takashi Ito and Shinji Okazaki' "review article Pushing the limits of lithography", Nature 406, 1027-1031 (2000).

[35] L. Novotny, R. Bian, and X. Xie, "Theory of nanometric optical tweezers", Physical Review Letters 79, 645-648 (1997).

[36] W. Zhang, L. Huang, C. Santschi, and O. J. F. Martin, "Trapping and sensing 10 nm metal nanoparticles using plasmonic dipole antennas", Nano Letters 10, 1006-1011 (2010).

[37] A. N. Grigorenko, N. W. Roberts, M. R. Dickinson, and Y. Zhang, "Nanometric optical tweezers based on nanostructured substrates", Nature Photonics 2, 365-370 (2008).

[38] J. A. Schuller, E. S. Barnard, W. Cai, Y. C. Jun, J. S. White, and M. L. Brongersma, "Plasmonics for extreme light concentration and manipulation", Nature Materials 9,193-204 (2010).

[39] H. A. Atwater and A. Polman, "Plasmonics for improved photovoltaic devices", Nature Materials 9, 865 (2010).

[40] E. J. Smythe, M. D. Dickey, J. Bao, G. M. Whitesides, and F. Capasso, "Optical antenna arrays on a fiber facet for in situ surface-enhanced raman scattering detection", Nano Letters 9, 1132-1138 (2009).

[41] N. Liu, M. Mesch, T. Weiss, M. Hentschel, and H. Giessen, "Infrared perfect absorber and its application as plasmonic sensor", Nano Letters 10, 2342-2348 (2010).

[42] G. Raschke, S. Kowarik, T. Franzl, C. Snnichsen, T. A. Klar, J. Feldmann, A. Nichtl, and K. Krzinger, “Biomolecular recognition based on single gold nanoparticle light scattering”, Nano Letters 3, 935-938 (2003).

[43] N. Liu, M. L. Tang, M. Hentschel, H. Giessen, and A. P. Alivisatos, “Nanoantenna enhanced gas sensing in a single tailored nanofocus", Nature Materials 10, 631-636 (2011).

[44] D. Bergman and M. Stockman, “Surface plasmon amplification by stimulated emission of radiation: Quantum generation of coherent surface plasmons in nanosystems", Physical Review Letters 90, 1-4 (2003).

[45] M. A. Noginov, G. Zhu, A. M. Belgrave, R. Bakker, V. M. Shalaev, E. E. Narimanov, S. Stout, E. Herz, T. Suteewong, and U. Wiesner, “Demonstration of a spaser-based nanolaser", Nature 460, 1110-1112 (2009).

[46] M. T. Hill, “Status and prospects for metallic and plasmonic nano-lasers", Journal of the Optical Society of America B 27, 36-44 (2010).

[47] S. W. Chang, C. Y. A. Ni, and S. L. Chuang, “Theory for bowtie plasmonic nanolasers", Optics Express 16, 10580-10595 (2008).

[48] K.-S. Lee and M. A. El-Sayed, “Dependence of the enhanced optical scattering efficiency relative to that of absorption for gold metal nanorods on aspect ratio, size, end-cap shape, and medium refractive index", The Journal of Physical Chemistry B 109, 20331-20338 (2005).

[49] S. E. Skrabalak, J. Chen, L. Au, X. Lu, X. Li, and Y. Xia, “Gold nanocages for biomedical applications", Advanced materials Deer field Beach Fla 19, 3177-3184 (2007).

[50] E. Boisselier and D. Astruc, “Gold nanoparticles in nanomedicine: preparations, imaging, diagnostics, therapies and toxicity", Chemical Society Reviews 38, 1759-1782 (2009).

[51] P.-J. Debouttire, S. Roux, F. Vocanson, C. Billotey, O. Beuf, A. Favre-Rguillon, Y. Lin, S. Pellet-Rostaing, R. Lamartine, P. Perriat, and O. Tillement, “Design of gold nanoparticles for magnetic resonance imaging", Advanced Functional Materials 16, 2330-2339 (2006).

[52] S. Lee, E.-J. Cha, K. Park, S.-Y. Lee, J.-K. Hong, I.-C. Sun, S. Y. Kim, K. Choi, I. C. Kwon, K. Kim, and et al., “A near-infrared-uorescence-quenched gold-nanoparticle imaging probe for in vivo drug screening and protease activity determination", Angewandte Chemie International Edition 47, 2804-2807 (2008).

[53] Silver S, *Microwave Antenna: Theory and Design*, New York: McGraw-Hill Book Co., 1949.

[54] E. M. Purcell, *"Spontaneous emission probabilities at radio frequencies"*, Phys. Rev. 69, 681 *(*1946*).*

[55] Lekner, John, *Theory of Reflection, of Electromagnetic and Particle Waves*, Springer,1987.

[56] R. E. Noskov, A. E. Krasnok and Y. S. Kivshar, " Nonlinear metal–dielectric nanoantennas for light switching and routing", New J. Phys. 14, 093005 (2012).

[57] A. Kuznetsov, A. Miroshnichenko, Y. Fu, J. Zhang, and B. Lukyanchuk, "Magnetic light," Sci. Rep. 2, 492 (2012).

[58] V. M. Shalaev, "Optical negative-index metamaterials," Nature Photon. 1, pp. 41–47, 2007.

[59] D. R. Smith, S. Schultz, P. Markos, and C. M. Soukoulis, "Determination of effective permittivity and permeability of metamaterials from reflection and transmission coefficients," Phys. Rev. B 65, 195104 (2002).

[60] U. Leonhardt, "Optical conformal mapping", Science 312, 1777–1780, 2006.

[61] J. B. Pendry, "Negative refraction makes a perfect lens", Phys. Rev. Lett. 85, 3966–3969 (2000).

[62] Q. Zhao, J. Zhou, F. Zhang, and D. Lippens, "Mie resonance-based dielectric metamaterials", Mater. Today 12 (2009).

[63] JN Reddy , *An introduction to the finite element method* , McGraw-Hill 2 (2.2), 1993

[64] B. Rolly, B. Stout, and N. Bonod, "Boosting the directivity of optical antennas with magnetic and electric dipolar resonant particles", Opt. Express 20, 20376–20386 (2012).

[65] M. Kerker, D. S. Wang, & C .L. Giles, "Electromagnetic scattering by magnetic spheres", J. Opt.Soc. Am. 73, 765–767 (1983).

[66] C. F. Bohren and D. R. Huffman, *Absorption and Scattering of Light by Small Particles*, John Wiley &Sons, New York, 1998.

[67] R. Gomez-Medina, B. Garcia-Camara, I. Suarez-Lacalle, F. Gonzalez, F. Moreno, M. Nieto-Vesperinas, and J. J. Saenz, "Electric and magnetic dipolar response of germanium nanospheres: Interference effects, scattering anisotropy, and optical forces", J. Nanophotonics 5, 053512 (2011).

[68] A. B. Evlyukhin, C. Reinhardt, A. Seidel, B. S. Lukyanchuk, and B. N. Chichkov, "Optical response features of si-nanoparticle arrays", Phys. Rev. B 82, 045404 (2010).

[69] M. Nieto-Vesperinas, R. Gomez-Medina, and J. S_aenz, "Angle-suppressed scattering and optical forces on submicrometer dielectric particles", J. Opt. Soc. Am. A 28, 54–60 (2011).

[70] A. Garcia-Etxarri, R. Gomez-Medina, L. S. Froufe-Perez, C. Lopez, L.Chantada, F. Scheffold, J. Aizpurua, M. Nieto-Vesperinas, and J. J. Saenz, "Strong magnetic response of submicron silicon particles in the infrared", Opt. Express 19, 4815–4826 (2011).

[71] A. B. Evlyukhin, C. Reinhardt, and B. N. Chichkov, "Multipole light scattering by nonspherical nanoparticles in the discrete dipole approximation", Phys. Rev. B 84, 235429 (2011).

[72] S. Staude, A. E. Miroshnichenko, M. Decker, N. T. Fofang, S. Liu, E. Gonzales, J. Dominguez, T. S. Luk, D. N. Neshev, I. Brener, and Y. Kivshar, "Tailoring directional scattering through magnetic and electric resonances in subwavelength silicon nanodisks", ACS Nano 7, 7824–7832 (2013).

[73] F. J. Bezares, J. P. Long, O. J. Glembocki, J. Guo, R. W. Rendell, R. Kasica, L. Shirey, J. C. Owrutsky, and J. D. Caldwell, "Mie resonance-enhanced light absorption in periodic silicon nanopillar arrays", Opt. Express 21, 27587-27601 (2013)

[74] E.palik, *Handbook of Optical Constant of Solids*, San Diago Academic, 1985.

[75] A. B. Evlyukhin, C. Reinhardt, E. Evlyukhin, and B. N. Chichkov, "Multipole analysis of light scattering by arbitrary-shaped nanoparticles on a plane surface", J. Opt. Soc. Am. B 30, 2589–2598 (2013).

[76] D. Sikda, W. Cheng and M. Premaratne, "Optically Resonant Magneto-Electric Cubic Nano antennas for Ultra-Directional Light Scattering", Journal of Applied Physics 117, 083101-083114(2015).

[77] C. H. Papas, *Theory of Electromagnetic Wave Propagation*, Courier Dover Publications, 2013.

[78] W. Liu, A. E. Miroshnichenko, D. N. Neshev, and Y. S. Kivshar, "Broadband unidirectional scattering by magneto-electric core–shell nanoparticles", ACS Nano 6, 5489–5497 (2012).